POLITECNICO DI MILANO

School of Industrial Engineering

Master of Science in
Mechanical Engineering

Design of a Space-Borne Quartz Crystal Microbalance

Advisor: Prof. BortolinoSaggin

Co-Advisor: Dr. Diego Scaccabarozzi

M.Sc.Thesis of

M.RezaSALEHI
Matr: 779399

Academic Year 2013-2014

Index

Table of Figures

Abstract

This work is focused on the mechanical design of the quartz crystal microbalance system. The microbalance holding system has been designed to assure the integrity of the sensor against the high vibration level foreseen during the instrument launch and landing on the mars surface. Mechanical design has been guided by the need of curtailing as much as possible the system resource request, assure convenient dynamic behavior and overcome high temperature differences of the environment.

The holding system is made by three springs and three supports, which also implements the electrical contact for the piezoelectric crystal.

Further on, this study also includes the design and optimization of vibration damping system for the quartz crystal microbalance. The damping system consists of an adaptable damper element whose main objective is to control the transmitted vibrations during the launch condition.

The environmental condition, have been simulated by the numerical and analytical models and the damping system has been designed to achieve the desired transmissivity.

Keywords : Quartz Crystal Microbalance, MR Damper, Smart Damper

1 Definition of Quartz Crystal Microbalance (QCM)

1.1 Introduction

Piezoelectricity is defined as electric polarization produced by mechanical strain in certain crystals the polarization being proportional to the strain. Curies first observed piezoelectricity in 1880 as a potential difference generated across two surfaces of a quartz crystal under strain.[1]

Lippmann predicted the converse piezoelectric effect and the deformation of a piezoelectric material by an applied electric field. Thus when a thin wafer from a piezoelectric crystal such as quartz is placed in an electric field of the right frequency it will oscillate in a mechanically resonant mode of the wafer.[2]

The resonance frequency depends upon the angles with respect to the crystallographic axis at which the wafer was cut from a single crystal and inversely on the crystal thickness. Figure (1-1) shows typical cut used to produce such wafers from a quartz single crystal. [3]

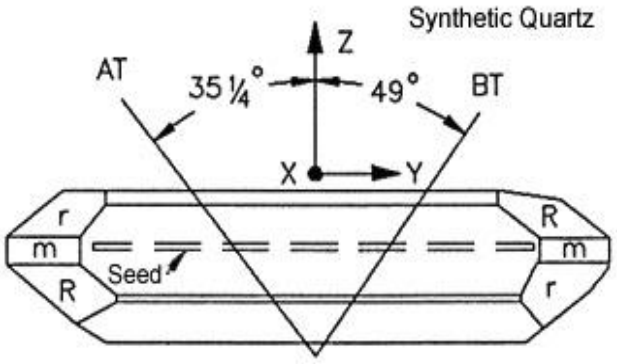

Figure 1-1 AT cut and BT cut Quartz Crystal

The angle most commonly chosen is referred to as the AT cut 35º15’ from the Z or optic axis of the crystal. AT cut angles are chosen so that temperature dependence of the resonant frequency is essentially zero at 25ºC.
These thin quartz plates with attached electrodes are called transverse shear mode resonators. Figure (1-2)

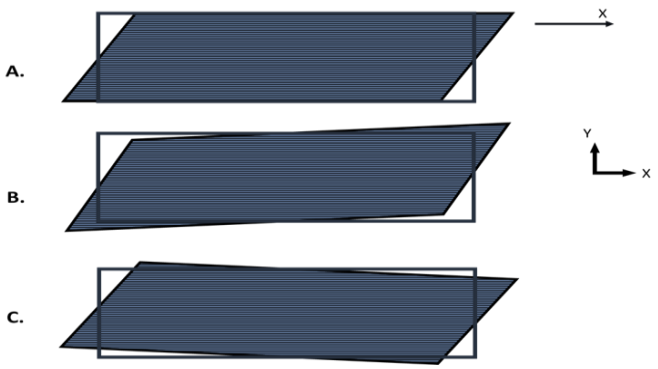

Figure 1-2 Natural Modes of oscillation of AT cut Quartz ,a).shear Mode

The development and applications of quartz plate TSM resonators are essential fields in electrical engineering. In the Early 1920’s the National Bureau of standards (U.S) began studies of quartz-crystal oscillators as frequency standards. [4]

To meet the growing demand for better accuracy, NBS sought outside partners, and began collaboration on oscillators with the naval research laboratory and Bell telephone Laboratories. In 1929 Bell labs delivered four complete temperature-controlled 100 kHz oscillators to NBS, and these oscillators quickly became the national primary standard of radio frequency.

By 1959 the facility involved a larger number of oscillators and the measurement uncertainty had been reduced to about 2 parts in 10 million.

An entertaining account of the history of the quartz crystal industry in the USA[5] indicates the critical role that quartz resonators played in the development of radio communications during World War II. Quartz resonators are presently found in many commercial products from quartz timepieces to ultra-stable frequency counters.

Quartz plate resonators have been used as sensitive microbalances for thin adherent films since the late 1950's, following the work of Sauerbrey[6], who coined the term Quartz Crystal Microbalance.
A quartz crystal microbalance consists of thin quartz crystal disk (natural or synthetic) with electrodes plated on it as shown in figure (1-3).

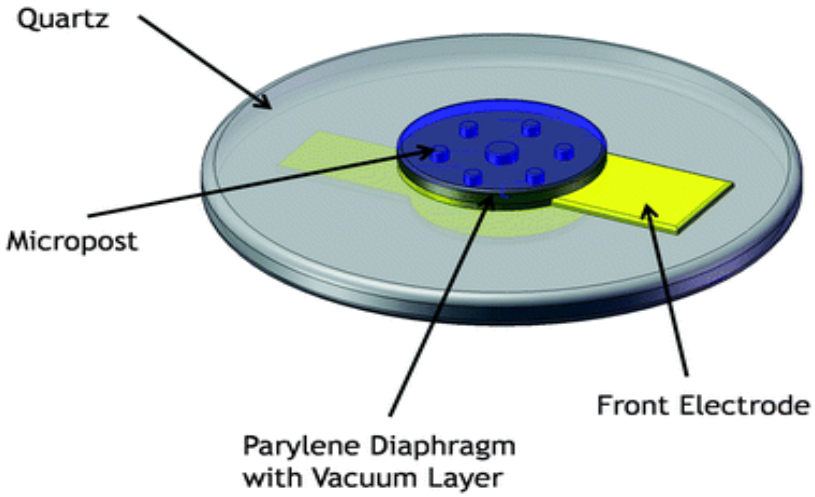

Figure 1-3 Quartz crystal Microbalance with mounted electrodes

1.2 Piezoelectric Crystals

The piezoelectric effect occurs only in certain types of crystals. There are 32 classes of crystals (I.E Cubic, Trigon and Orthorhombic) of which 20 classes exhibit the piezoelectric effect[7]. The piezoelectric property exists only in ionic crystalline solids that crystallize in structures lacking a center of inversion. The center of inversion is the point about which the crystal is symmetrical.

The piezoelectric effect is excluded for all crystals with a center of symmetry.[8] Piezoelectric crystals are used to control and manage the frequencies of the carrier signals used in electric communications.

Among the crystals, which exhibit the piezoelectric effect, quartz alone provides the necessary combination of mechanical, electrical, chemical and thermal properties required for making piezoelectric elements for the electrical communication field. [9]

The quartz crystal unit provides a coupling between the mechanical resonance frequency of the crystal and the electric circuit and therefore, can be used as an electromechanical transducer.

The coupling between the mechanical properties of the quartz and the electric circuit occurs through the piezoelectric effect. The piezoelectric effect occurs because of the generation of dipoles in crystals upon the application of an electric field. Figure (1-4)

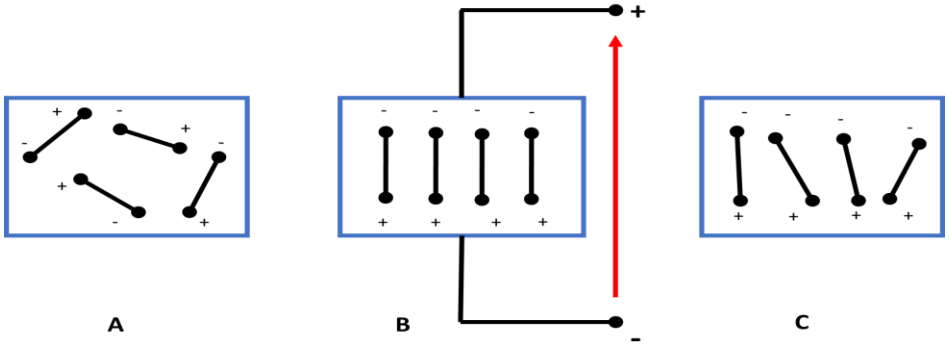

Figure 1-4 Electric dipole moments and Polarization

(a) before, (b) during , (c) after the polarization

A piezoelectric crystal is a precisely cut slab from a crystal of quartz. The crystal s are cut at specific angle and modified to suppress the unwanted modes. There are several types of crystal cuts such as AT-cuts, BT-cuts crystals and SC-cuts crystals. The crystals differ in the angle of cut.

The application of an electric potential to a quartz crystal produces internal mechanical stress. In quartz crystals an applied pressure deforms the crystal lattice and causes separation of positive and negative charge, generating a dipole moment in each crystal cell.
When a quartz crystal is connected to a periodic voltage source, the crystal vibrates at the frequency of the exciting voltage. The vibration causes the contraction or elongation of the crystal parallel to the direction of the applied electric field.

If the frequency of the voltage source is close to one of the mechanical resonant frequencies of the quartz crystal, resonance occurs and the amplitude of the vibration reaches a maximum. A piezoelectric quartz crystal has many modes of resonance.
The mode of vibration, which is most sensitive to the addition or removal of mass for a quartz crystal,is called the high frequency thickness shear mode.
For the crystal to oscillate in the thickness shear mode, the crystal must be cut to give a specific orientation with respect to the crystal axes.
Crystalline quartz is composed of two elements, silicon and oxygen and the chemical formula is SiO2.

The amorphous from SiO2 is a major constituent of many rocks and many sands. The crystalline for of SiO2 or quartz is relatively abundant in nature, but not in the highly perfect form required for the manufacture of quartz crystal units.

Most of the high quality crystals of naturequartz are from Brazil. Natural quartz crystals are grown from water solutions containing dissolved SiO2; silicon dioxide is highly soluble in water at ordinary temperatures. However the solubility increases in alkaline solutions.
Crystal of cultured quartzis grown by dissolving SiO2 in an alkaline solution of water at the temperature near to the critical temperature of the quartz. Autoclaves which can withstand pressures exceeding $1.01 * 10^8$Pa are required for the preparation of the cultured quartz crystal.

The differences between the samples of quartz are due to the crystalline imperfections. The crystalline form of SiO2 below 573 ºC is called Alpha Quartz[10].

Piezoelectric quartz crystal has five important properties:

1. The piezoelectric effect provides a coupling between the electrical circuit and the mechanical properties of a crystal.
2. The internal dissipation is low.
3. The density and elastic constants of the crystals are uniform, so that a crystal cut at a given orientation will always have the same frequency behaviour.
4. Crystals cut at a specific orientation have advantageous properties.
5. The crystals have a small frequency change with temperature and will be free from secondary modes of motion.[11]

Resonance can occur in quartz crystals at different frequencies. Resonance in crystal resonators occur at all the frequencies where mechanical displacements of the elastic medium from standing wave patterns. In resonators terminology, these patterns are called resonance modes of motion.

The simplest mode pattern occurs at the fundamental frequencies of the low frequency resonators. Since no vibrating system is frictionless, energy must be supplied to sustain oscillations, even in the case of crystal vibrations the energy is supplied to the vibrating crystal through the piezoelectric effect.

In crystal oscillations, the energy losses are extremely small. The properties of quartz, which make quartz the most satisfactory material for frequency stabilization, are hardness, low internal dissipation, durability, uniformity, freedom from flaws and temperature independent resonant frequencies. There are other crystals which satisfy the above requirements but none with the exception of the quartz that satisfy all of them

.

1.3 Sauerbrey Theory

In 1959 Sauerbrey demonstrated the dependence of the changes in fundamental frequency of response on the mass accumulated on the crystal. In his work Sauerbrey assumed that, for small vibrations, the increase of the mass could be seen as the effect caused by a thin additional layer. The Sauerbrey's model represents an oscillating quartz having mass M_q and thickness t_q figure (1-5)

Part (a) of figure (1-5) shows the oscillation of a bare quartz crystal oscillating in its fundamental thickness-shear mode. The dotted lines in part (a) and part (b) of figure (1-5) represent the shear waves in quartz crystal.

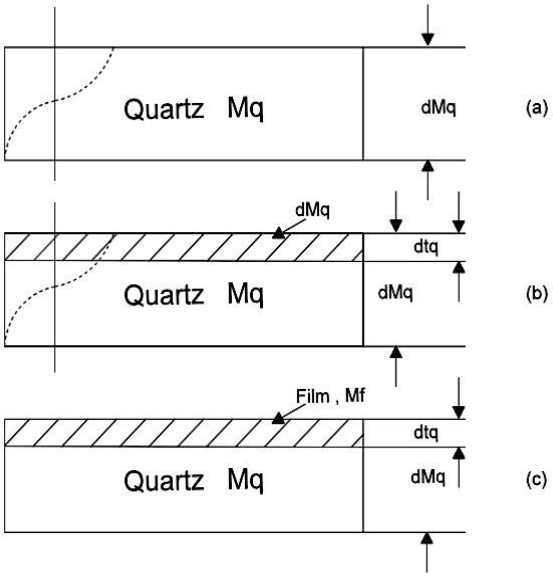

Figure 1-5 Schematic representation of Sauerbrey's model

For the quartz crystal to oscillate in thickness-shear mode the thickness of the crystal should be exactly half of the wavelength of the shear-mode elastic waves in the thickness direction.
This condition can be mathematically represented as

$$t_q = \frac{\lambda_q}{2} (1.1)$$

The resonance frequency is

$$f_q = \frac{V_q}{\lambda_q} = \frac{V_q}{2t_q} (1.2)$$

Where λ_q is the length of the acoustic wave that propagates in the quartz that is equal to twice the thickness of the quartzt_q ,V_q is the speed of propagation of the wave and it is equal to $\lambda_q * f_q$.

When there is a deposition of mass (dM_q) on the quartz surface, the thickness of the quartz increases (dt_q) and the resonance frequency (df_q) decreases:

$$\frac{df_q}{f_q} = -\frac{dt_q}{t_q} \qquad (1.3)$$

$$\frac{df_q}{f_q} = -\frac{dM_q}{M_q} \qquad (1.4)$$

The oscillation of the crystal under these conditions is shown in part (b) of figure 1.5. Sauerbrey assumed that:

1. The material coated on the crystal is perfectly bound to the electrode.
2. The material coated on the crystal is elastic and does not undergo viscoelastic deformations during oscillation.
3. The thickness of the coated material is uniform over the crystal surface.
4. The acoustic impedance of the crystal is identical to that quartz.

All the above conditions can be satisfied when the material thickness is small compared to the quartz plate thickness.[12]

Sauerbrey obtained the fundamental equation for microgravimetric applications depositing the films on the surface of quartz. This equation is derived from the combination of the two previous equations:

$$\frac{df_q}{fq} = -\left(\frac{2f_q}{\rho_q V_q A}\right) dM_q \quad (1.5)$$

Where A is the Area of the surface of the crystal, expressed in cm^2 ,ρ_q is the density of the quartz (equal to 2648 g. cm^{-3}) and V_q is the speed of propagation of an acoustic wave in the quartz (equal to 3,336 * 10^5 $cm.s^{-1}$) so substituting the values :

$$df_q = -2.26 * 10^{-6} f_q^2 \frac{dM_q}{A} \qquad (1.6)$$

The thickness of the crystal, for the same area A, determines the resonance frequency and hence the sensitivity of the mass deposited, the lower limit to the thickness is imposed by the intrinsic fragility of the quartz. The previous formulas are valid under the assumptions of a uniform distribution of the mass on the crystal in the film.

These equations provide semi-quantitative descriptive analysis: in fact there are factors with a strong influence on the accuracy of measurement, such as the damping in the electrical and environmental temperature, so the necessary calibration curve must be used to get good quantitative results. The calibration curves are obtained inserting the quartz crystal in an oscillating circuit. The resonant frequency of the system, in comparison with the frequency of the system, in comparison with the frequency of a reference crystal, is detected using a frequency meter.

Stockbridge [13]employed a perturbation analysis and arrived at the same result as described mathematically in equation 1.5. He assumed that the acoustic wave does not propagate in the film. The basic assumption made by Stockbridge is that the amount of potential energy stored in the deposited foreign layer during oscillation is negligible. This restricts the use of linear mass-frequency relationship to small film thicknesses with negligible shear deformation [14]. Sauerbrey has tested equation 1.5 by evaporating thin metal films onto quartz crystal and monitoring the change in frequency.[15]

In QCM AT-Type devices, the acoustic waves propagate in a direction perpendicular to the crystal surface. When the frequency of the oscillation closely approximates to the fundamental frequency, the resonance is reached. As it has been seen, the resonance frequency depends on the thickness, the shape and the mass of the quartz.

Other factors that influence the frequency variation are, for example, the temperature (T), the mass (m), the viscosity (μ) and the humidity (H) of the liquid or gaseous adjacent media.[16] Thus

$$\Delta f = \frac{\partial f}{\partial m}\Delta m + \frac{\partial f}{\partial \mu}\Delta \mu + \frac{\partial f}{\partial T}\Delta T + \frac{\partial f}{\partial H}\Delta H \qquad (1.7)$$

The knowledge of the amplitude distribution on the crystal surface is important for the analysis of the mass load sensitivity of the quartz crystal when used as a thin-film thickness monitor. [17] The displacement of a point, vibrating with simple harmonic motion may be decreased as

$$x = A.Sin(\varpi t) \qquad (1.8)$$

Where A is the vibrational amplitude in that point and $\varpi = 2\pi f$ is the angular frequency. Earlier experimental results in gas and vacuum indicated that the vibration amplitude in the center of a quartz resonator is in the range from 10 nm to 200 nm.
Deposition of a thin film on the crystal surface decreases the frequency in proportion to the mass of the film. A resonant oscillation is achieved putting the crystal into an oscillating circuit where the electrical and mechanical oscillators are close to the fundamental frequency of the crystal.

The fundamental frequency depends upon the thickness of the wafer, its shape and its mass. Some factors can influence the oscillation frequency, like the thickness, the density and the shear modulus of the quartz that are constant, and the physical properties of the adjacent media. As shown by Sauerbrey, changes in the resonant frequency are simply related to the mass accumulated on the crystal. Thus for detection of particles in air, the frequency change is simply related to the change in mass:

$$\Delta f \propto K\Delta m$$

Sauerbrey originally realized that the frequency decrease was proportional to the mass deposited over the crystal. For small mass charges the decrease in a thickness shear mode frequency of a crystal upon which a thin film is deposited is linearly proportional to the deposited mass. The linear mass – frequency relation is valid up to a mass load of 2%.[18]

In addition the linear mass-frequency relation was found to be valid until the frequency decrease due to the loading is approximately 2% of the unload frequency. Beyond that range, the relation between the frequency decrease and the mass loading is non linear, because the acoustic impedance of the coated film will be different from the acoustic impedance of quartz.[19]

The prediction of the maximum mass load a quartz crystal can accommodate before it fails to oscillate is difficult because it depends on many factors such as the quality of the quartz crystal, the acoustic losses in the coated material, the stresses generated in the crystal by the deposited material and the design of the crystal holder and oscillator circuitry.[20]

1.4 Sensitivity of the Quartz Crystal Microbalance (QCM)

The sensitivity of the quartz crystal microbalance is not uniform over its surface. A quartz crystal resonator with a finite size and contoured surface does not have a uniform mass sensitivity over its entire surface. The mass induced frequency change will depend on upon the position of the deposited mass on the crystal surface. The differential mass sensitivity was found to be reaching a maximum at the center of the crystal and reduced to zero just slightly beyond the boundary of the electrode.

In the equivalent circuit, the resistance increases as more material is deposited onto the crystal. The resistance increase is due to the increase in the acoustic losses in the coated material.[21]
Jose Et Al. studied how the diameter of electrodes, influence the mass sensitivity of the microbalance. The radial dependence of mass sensitivity of the sensing surface is analytically calculated for examples of “Modified electrode” quartz crystal resonators (QCR).

The term “modified electrode” QCR is used with respect to the conventional QCR, which has two identical circular and concentric electrodes. They conclude that the difference in sensitivity becomes insignificant if the sensing area increases beyond a diameter of 7 mm.[22]

Figure (1-6) shows how the mass sensitivity varies in function of the radius of the electrodes. The first number (n) is the diameter of the upper electrode and 2nd number (m) is the diameter if the lower electrode.

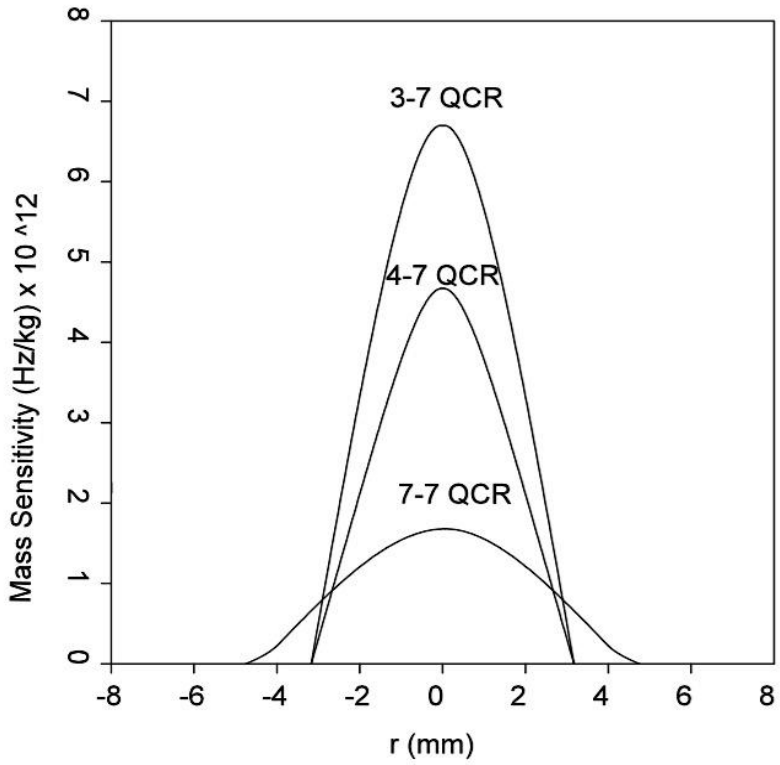

Figure 1-6 Calculated radial dependence of the differential mass sensitivity for 3 nm type electrode.

1.5 Equivalent circuit of the quartz resonator

The behavior of the crystal oscillating near series resonance is often represented using the Butterworth-Van Dyke electrical model, as shown in figure (1-7)

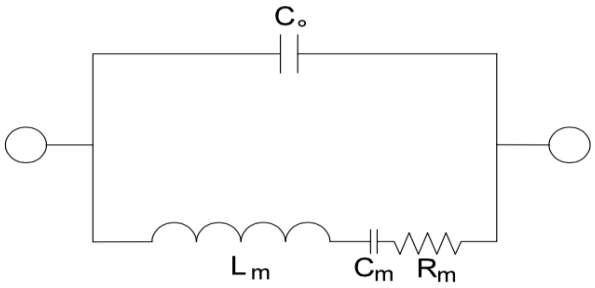

Figure 1-7 Butterworth-van Dyke electrical model for a quartz crystal oscillating near series resonance.

If an ideal quartz crystal (i.e.no resistor/frictional losses) is subjected to an AC voltage and the current is then removed, the stored inertial and elastic energies of the crystal would lead to continuous oscillation. Likewise, in an ideal circuit, energy oscillates between the inductor, which stores the energy in the form of a magnetic field, and the capacitor, which stores energy in the form of electrical potential.

The inertial energy of the quartz crystal relates to the inductor (L_m) and the elastic energy related to the capacitor (C_m). Maximum surface displacement of the crystal corresponds to a fully charged capacitor in which the potential energy is at the maximum. Zero surface displacement of the crystal corresponds to a maximum field around the inductor and maximum current, i.e. the point of maximum kinetic energy. However the quartz crystal is not ideal (there are frictional losses, which may be linked to a resistor).

The motional resistance (R_m) therefore increases with viscosity of the surrounding medium. Together the inductor, resistor and the capacitor are placed in series because they are directly affected by the piezoelectricity of the quartz. Parasitic capacitance, (C_o) is also present in parallel and arises from the crystal holder, mounting structures cables, etc. placing the crystal in an oscillator circuit allows easy determination of the resistance through impedance analysis.

An automatic gain control amplifier, in which the voltage is supplied in such a way, can drive the QCM crystal that the circuit oscillates at a frequency for which the phase shift around the loop is 0°. By nulling C_0 and recognizing that the reactance of the capacitor and inductor cancel at series resonance is function of the frictional losses of the medium contacting the crystal surface, it is useful for detecting phase changes, the creation of networks, and relative viscoelastic properties of the film bound to the crystal surface.[2324]

1.6 The temperature coefficient of frequency for quartz crystals

The frequency of any resonator depends on its thickness, density and the elastic constant and each of these changes with the temperature.

Therefore the frequency of any resonator is usually temperature dependent, however the frequency of an AT-cut quartz crystal is not a function of a temperature trough a convenient balancing of the properties of the crystal. For an infinite plate vibrating in thickness mode, the resonant frequency is given by:

$$f_n = \frac{n}{2e}\sqrt{\frac{Cij}{\rho}} \qquad (1.9)$$

Where :

e= thickness of the plate

$\rho =$ density of the quartz

Cij= ratio of the stress to the strain associated with the elastic wave which is being propagated in the quartz.

Assuming linear temperature dependence of the above variables, the linear temperature coefficient of the frequency, T_{ft} is given by :

$$T_{ft} = \frac{1}{f}\cdot\frac{df}{dT} = -\frac{1}{e}\cdot\frac{de}{dT} - \frac{1}{2}\cdot\frac{1}{\rho}\cdot\frac{d\rho}{dT} \qquad (1.10)$$

Since quartz expands during heating, $\frac{d\rho}{dT}$ is negative.

The change in thickness with temperature is $\frac{de}{dT}$ and is a positive quantity .

T_{ft} can be made zero by balancing out the effects of temperature on density and elastic modulus so that the temperature dependence of frequency can be minimized.

This balancing out of the effects is possible in AT-cut quartz crystals. For most other crystals it is impossible to find any orientation with zero temperature coefficient.[25]

1.7 QCM response in liquids

Since the mid 1980's [26]it has been recognized that TSM resonators can also operate in fluid media if electronic oscillator drivers of suitable gain are employed to excite the resonator and to overcome the losses due to damping of the resonator by the fluid. The oscillation of quartz crystals in liquids is contrary to the belief that the viscous losses to the liquid would suppress the oscillation of the crystals.[27]

The concept of an acceleration dependent mass sensitivity can explain why the frequency of a shear vibrating quartz crystal resonator, in contact with a liquid, depends on the viscosity of the liquid. The frequency change, when one face of a quartz crystal resonator is in contact with a liquid with density ρ and viscosity μ, was first calculated by Kanazawa and Gordon in 1985 and later using the Energy Transfer Model :

$$\Delta f = - f_q^{\frac{3}{2}} \left(\frac{\rho_1 . \mu_1}{\pi . \rho_q . \mu_q} \right) \qquad (1.11)$$

Where ρ_q and μ_q are the quartz density and shear modulus, respectively. This relation has been experimentally tested by [28]with a 30 MHz quartz crystal.
When such a resonator is in contact with a liquid and this is a common situation in many applications of the QCM, the vibration amplitude, and also the acceleration, decay exponentially from the crystal surface into the liquid. In liquids, the amplitude of oscillation of the quartz crystal decreases because the liquid viscosity and the liquid density increase the shear stress on the crystal.

The amplitude of oscillation is proportional to the net driving force on the crystal. The net driving force is equal to the difference between the piezoelectric force and the shear stress because the shear stress reduces the net force on the crystal[29]. Any mass accumulated on a crystal oscillates synchronously with the crystal surface and reduces the resonant frequency of the crystal. When the crystal surface is in contact with a liquid, a thin layer of liquid adjacent to the oscillating crystal is entrained by the crystal surface, further reducing the frequency of the crystal.[30]

The oscillating crystal sets up an oscillating liquid boundary layer adjacent to the face in contact with the liquid. So mass accumulation on the surface and liquid contact both lead to a decrease in the resonant frequency of the crystal. The sensitivity of the resonant frequency of the crystal to liquid properties can be used in monitoring the liquid density and viscosity.

Yao and Zhou studied the effect of the properties of the liquids on the oscillation of quartz crystals. They found out that, for a crystal immersed in a liquid there exists a critical temperature below which the crystal ceases to oscillate. The temperature at which the crystal ceases to oscillate differs for different crystals even with the same rated frequency. They concluded that the crystals oscillate with greater difficulty in concentrated solutions and in liquids with high molecular weight.

They also compared the effects of density and viscosity of the liquids on the frequency behavior the crystals and concluded that the influence of the density is more significant than the influence of viscosity on the frequency of the crystals.[31] Nomura and Okuhara performed experiments with quartz crystals in various liquids and suggested an empirical equation that relates the frequency shifts of the crystals to the density and viscosity of the liquid. They also indicated that the crystals did not oscillate in some of the liquids tested.[32]

1.8 Stress effects in quartz crystals

The frequency of vibration of a quartz crystal depends on the dimensions of the quartz crystal, the density of the quartz crystal and the elastic stiffness of the quartz crystal. All three quantities vary when there is static stress or initial stress present in the quartz crystal. The resonant frequency of the crystal changes with static stress. Two main sources of static stress are : mechanical sources just like electrodes and thermal shocks arising from ambient temperature changes. Quartz crystal microbalances can also be used for measuring the stress effects in thin films that result from film deposition, sputtering, ion implementation or chemical reactions in thin films. The magnitude of stress effects in a quartz crystal may be or may not be important in given situation.The stresses arising from materials on the surface of the quartz crystal are shown in the figure (1-8). In normal usage of a quartz crystal as a microbalance, changes in the resonant frequency are observed due to mass changes on the surface of the crystals.

When the stress is built in the thin film on the surface of the crystal, there is a net force per unit width acting across the thin film and quartz interface that stress biases the quartz.
The frequency changes caused by this stress bias are referred to as the "stress effects".

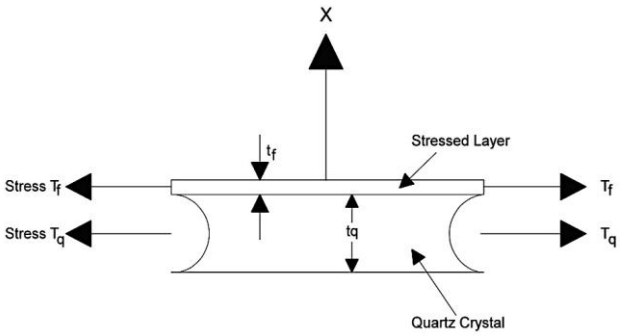

Figure 1-8 Stresses in quartz crystal after coating

The force per unit width acting on the quartz crystal is related to the lateral stress in the deposited thin film. The lateral stress may be the intrinsic stress arising in the thin films due to the nucleation process. (i.e. a process which occurs before the growth of the films on the crystal surface). The lateral stress can increase during sputtering or ion implantation.

When the bombarding particles strike the surface of the already deposited film during the film growth (i.e. by sputtering or ion implantation), the bombarded layer can have lattice structural damage. When the bombarded layer tries to expand or contract from the structural damage, the lateral stress can increase. Sputtering and ion implantation are two different types of procedures by which metallic films are grown.

A lateral stress can also arise from the free volume changes associated with chemical reactions in the coated film. The force per unit width in N/m is given by S_f the integral through the film thickness,

$$S_f = \int_0^{tf} S_f \, dx \qquad (1.12)$$

Where t_f is the thickness of the deposited film that has the lateral stress, x is the coordinate normal to the quartz resonator surface, and T_f is the lateral stress in the deposited film.
According to the Newton's law, there must be an equal and opposite force per unit width acting at the interface from the quartz resonator side. This results in a lateral stress T_q in the quartz. Assuming a uniform lateral stress, the lateral stress T_q in the quartz resonator is given by

$$T_q = -\frac{S_f}{t_q} \qquad (1.13)$$

Where t_q is the thickness of the quartz crystal. This is the stress bias that changes the resonant frequency of the quartz crystal. According to the sign convention, a positive value of T_q means tension in the quartz resonator. The presence of negative sign in equation 1.13 is because the stress in the quartz resonator would be opposite to the stress in the thin film.

The frictional frequency change$\left(\frac{d_{fs}}{f}\right)$due to the lateral stress in the quartz resonator is given by [33]:

$$K.T_q = -\frac{d_{fs}}{f} \qquad (1.14)$$

Where (K) is a constant for a given crystallographic orientation of the quartz crystal. The two most commonly used crystals are the AT-cut and the BT-cut quartz crystals. The parameter K has the values of $2.75*10^{-11}$ and $2.65 * 10^{-11} m^2/N$ for the AT and BT cut crystals respectively.

1.9 Gallium Orthophosphate GaPO4

Gallium phosphate (GaPO4, also gallium orthophosphate) is a piezoelectric crystal material Homeotic to quartz (SiO2) where half of the Si atoms, each with four valance electrons, are replaced alternately by Ga and P atoms with three and five valence electrons, respectively thereby doubling the piezoelectric effect.[34][35] Contrary to quartz, GaPO4 is not found in nature. Therefore a hydrothermal process must be used to synthesize the crystal.

Some material constants are similar to quartz thus GaPO4 can be used for all quartz applications without changes in the arrangement of the device. But the well known $\alpha - \beta$ phase transition, which changes the structure in SiO2, is absent in GaPO4, thus the novel crystal can be used up to 970°C where another phase transition occurs and the low quartz structure is changed into a cristobalite like one. The most physical properties of the material are very stable up to at least 900°C. (figure 1-9)

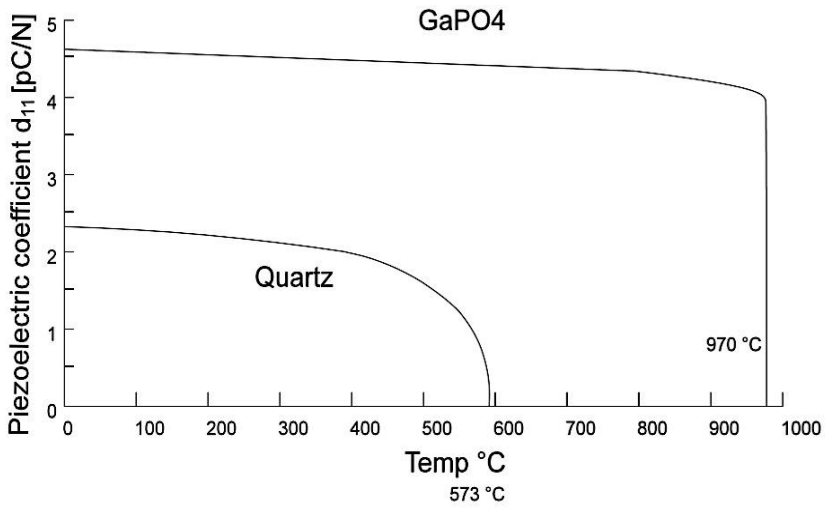

Figure 1-9 Piezoelectric constant of quartz and GaPO4

Due to the high thermal stability (up to 700°C) and the high sensitivity of the single crystalline GaPO4, make it very attractive choice for a wide range of uncooled high temperature applications. GaPO4 offers good temperature compensation for a new generation of crystal microbalance operating at temperatures up to at least 700°C.

Recently piezoelectric quartz crystal has found widely applications in chemical and bio sensor as quartz crystal microbalance (QCM) techniques. The quartz crystal of AT-cut used for the QCM method. This cutting mode of the quartz crystal device shows a good temperature compensated behavior of the resonant frequency around room temperature, but the maximum operating temperature is limited due to the phase transition near 570°C. for this weak point, QCM technique limited low temperature applications under 200°C.

This indicates clearly a larger possible measuring range for the GaPO4 resonator for microbalance applications that it is possible with the QCM.[36] These outstanding properties make GaPO4 very suitable for microbalance applications like affinity sensors for biological investigations or microbalances for very sensitive particulate measuring systems. Other advantages against quartz are the doubled piezoelectric coefficient d_{11} and thus the higher electric mechanical coupling coefficient 'k'.

The higher density (3570 kg/m^3) leads to a lower acoustic velocity and thus to a lower thickness of a resonator with the same frequency.
First measurements on GaPO4 resonators were published 1989 [37] and because of the low material quality results were poor. Much effort has been done to increase the material quality and the manufacturing process on GaPO4 resonators.[38]

Another necessary material properties is the electrical insulation. Most materials, for example some kinds of ceramics, have a high insulation, but for higher temperatures (more than 500°C) the insulation drops down and thus the quality factor of the resonator. The resistivity of GaPO4 is shown in figure(1-10). At 900°C the resistivity is still higher than 1 MΩ.

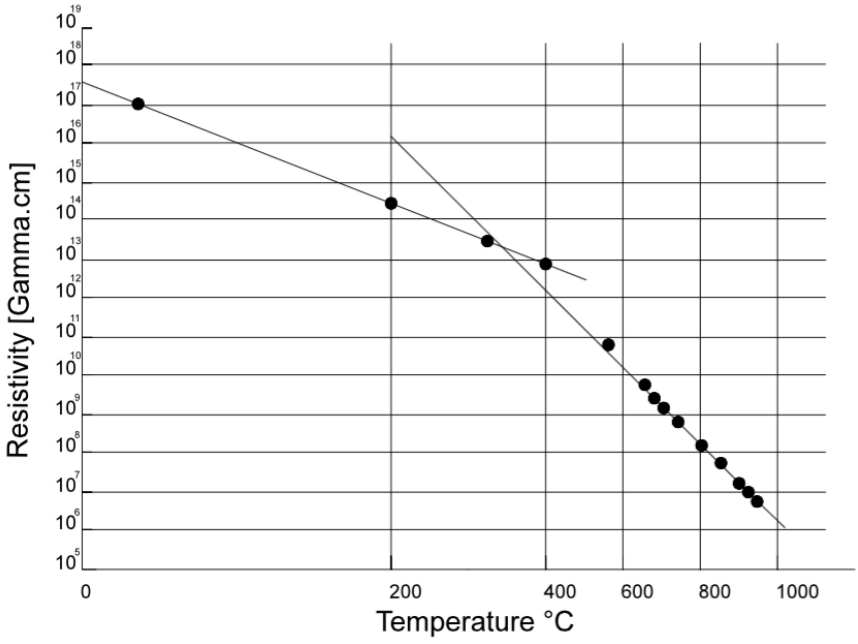

Figure 1-10 Resistivity of GaPO4 depending on temperature

Different experiments were done by Thanner Et Al. to demonstrate the advantages of a crystal microbalance based on GAPO4. In these experiments the GaPO4 resonator was used for film thickness determination and compared with a commercial QCM demonstrating that using GaPO4 resonators instead of quartz the measuring range can be extend.[39]

1.10 Operating Principle

Depending on the way a piezoelectric material is cut, three main types of operations can be distinguished: 1.Transversal 2.Longtudinal 3.Shear.

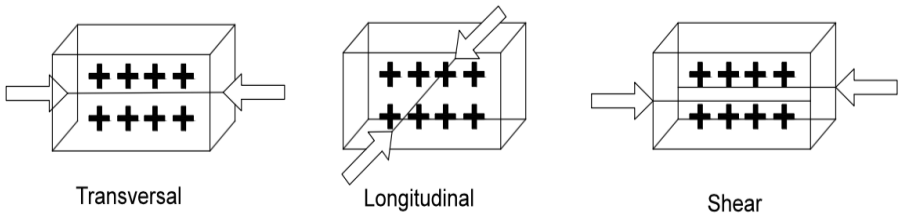

Figure 1-11 Gallium phosphate sensing elements

A Gallium Phosphate crystal is shown with typical sensor elements manufactured out of it. Depending on the design of a sensor different "modes" to load the crystal can be used: transversal, longitudinal and shear. (arrows indicate the direction where the load is applied.) Charges are generated on both "x-sides" of the element. The positive charges on the front side are accompanied by the negative charges on the back.

Transverse Effect: Force is applied along the neutral axis and the charges are generated along the d_{11} direction. The amount of charge depends on the geometrical dimensions of the respective piezoelectric element. When dimensions a,b,c apply :

$$C_y = -d_{11} \cdot F_y \cdot \frac{b}{a} \qquad (1.15)$$

Where b is the dimension in line with the neutral axis and a is in line with the charge generating axis.

Longitudinal Effect: The amount of charge produced is strictly proportional to the applied force and is independent of size and shape of the piezoelectric element. Using several elements that are mechanically in series and electrically in parallel is the only way to increase the charge output.

The resulting charge is :

$$C_x = d_{11} \,.\, F_x \,.\, n \qquad (1.16)$$

Where

d_{11} is piezoelectric coefficient [pC/N],

F_x is applied Force in x-direction [N]

n is the number of elements.

Shear Effect :

Again, the charges produced are strictly proportional to the applied forces and are independent of the element's size and shape. For 'n' elements mechanically in series and electrically in parallel the charge is:

$$C_x = 2 \,.\, d_{11} \,.\, F_x \,.\, n \qquad (1.17)$$

In contrary to the longitudinal and shear effect, the transverse effect opens the possibility to fine tune sensitivity depending on the force applied and the element dimension. Therefore piezo-crystal sensors almost exclusively use the transverse effect since it is possible to reproducibly obtain high charge outputs in combination with excellent temperature behavior.

1.11 Principle of Microbalance with GaPO4

A microbalance based on GaPo4 consists of the same elements like another microbalance. In principle the frequency and the damping of the resonator are changed because of the loading. The loading is in the simplest case a rigid layer, which leads to a shift in frequency because of the increased mass.

$$\Delta f_R = -2 \,.\, m \,.\, f_R^{\,2} \Big/ \sqrt{\rho \,.\, C_{eff}^{D}} \qquad (1.18)$$

Where ρ and C_{eff}^{D} are density and elastic constant of GaPo4. GaPO4 is a very promising material for microbalance application. Advantages are expected especially in high temperature applications or in applications where a high coupling coefficient is necessary. A first demonstration was shown with GaPO4 as affinity sensor and another application is in progress where particulates can be analyzed by the use of thermogravimetry[40].

Gallium phosphate is a piezoelectric crystal, which has been developed for the production of pressure transducers allowing miniaturization and high thermal stability without cooling while maintaining high sensitivity and accuracy.

The crystal lattice is stable and the piezoelectric coefficient remains at a high level up to a reconstructive phase transition at 970°C[41]. GaPO4 has been used for the production of pressure transducers for seven years now and the manufacturing experiences together with today's crystal growth facilities helped to make it available for a lot of different application.[42]

1.12 Micro-thermogravimetric device

The micro-thermogravimetric device consists of an oscillating quartz crystal microbalance with an integrated micro-heater that might turn out to be extremely useful in the study of the desorption of volatile compounds from refractory materials. Zinzi et al. performed an experiment by studying the release of absorbed water from clay.
Clay has been principally chosen because it is a material known for its ability to desorb and subsequently re-adsorb water at low temperatures and it might be considered a test mineral for a large number of applications, from first guess analysis of agricultural soil to quick inspection of materials of planetological interest. Results show that the device can be in stable operative conditions at 100°C with 0.5W of power supplied, allowing to measure the amount of desorbed water.

The very compact device here presented (hereafter called HQCM – heated QCM) consists of a QCM with an integrated micro-heater. Figure (1-15)
The micro-thermogravimetric device consists of an oscillating quartz crystal microbalance with an integrated micro-heater that might turn out to be extremely useful in the study of desorption of volatile compounds from refractory materials. Zinzi et al. performed an experiment by studying the release of adsorbed water from clay.

It is designed to perform micro-thermogravimetric ($\mu - TG$) analysis and taking into account its low mass and power requirements, it is ideal for applications in several fields, as for example in low space missions of planetological interest like Volatile in situ thermal analyzer.[43]

1.13 Objective of the thesis

The objective of this study is to design a holding system based on assumptions, consideration, design limits and the evaluated data and results that have been prepared up to now.

Finding out a type of material with low density, low thermal conductivity coefficient, which provides also a low weight and durable holding system, that is compatible with the cryogenic temperatures intervals is the first step of this study.

The optimum configuration of the holding system, position of the support and springs, sizing and dimensioning of the elements, mounting methods and joints, and finding the best assembly algorithm is the next step of this effort.

Recognition and identification of the mechanical vibration by which the instrument is subjected during the launching of spacecraft and simulating the proportionate effect of the applied noise using mathematical methods and finding out a possible solution to prohibit these effects.

Design and manufacturing of damping system by which it is possible to inhibit the surrounding blasts and certify its appropriate action is the last step of this effort.

2 Mechanical Design of Supports and Holdingsystem

2.1 Design Requirements:

The holding system is designed in order to reduce as much as possible the weight of the system. Also the total height of the holding system (support and the spring) is reduced as much as possible in order to be lower than 18 mm. As design constraint, the first natural frequency of the structure must be greater than 1kHz and the radial overall dimensions must be reduced as much as possible.

The stiffness of the springs and supports depends mainly on their thickness so the determination of the minimum thickness of the supports is a critical step of the design phase.

In order to have *First Natural Frequency* greater than 1kHz, the thickness of the elements must be high so as to increase the stiffness of the system but on the other hand, a high stiffness would lead to high stiffness level due to the expected thermal environment, being temperature working range within -200°C to 150°C.

A proper clamping system has to be designed to prevent the movement of quartz under the acceleration of $500 m/s^2$. The clamping system must also ensure the mechanical resistance of the quartz during the vibration.

Figure (2-1) shows a sketch of the holding system conceived to satisfy design constraints. Quartz would be supported by three elastic elements with stiffness k, hereafter named supports that provide stiff connection and thermal insulation.

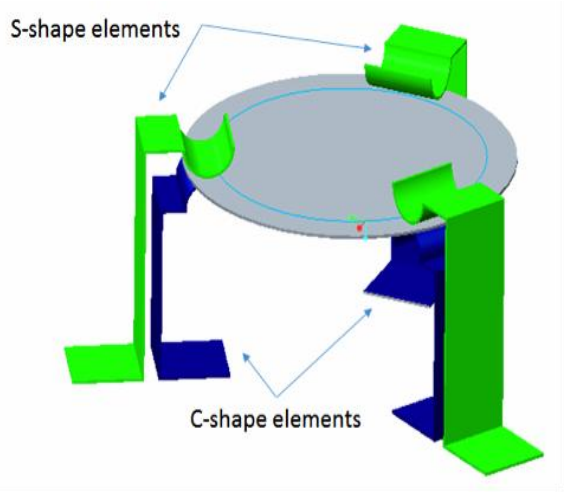

Figure 2-1 Microbalance Model

Quartz is held against movements due to external acceleration by three additional elastic elements, hereafter called springs, whose preloading provides required force against sliding. These supports do not have only the function of firmly holding the microbalance, but they are also designed in order to constitute the electrical contacts.
The crystal supports design is therefore driven by the following requirements:

2.1.1 Identify and Prevent buckling phenomenon

Among all the characteristics and design considerations of the holding system to inhibit the buckling phenomena is one of the most important issue.Buckling is characterized by a sudden sideways failure of a structural member subjected to high compressive stress, where the compressive stress at the point of failure is less than the ultimate compressive stress that the material is capable of withstanding.
Analyses of buckling often make use of an artificial axial load eccentricity that introduces a secondary bending moment that is not a part of the primary applied force. As an applied load is increased on the support, it will ultimately become large enough to cause the supoort to become unstable and is said to *have buckled*.

2.1.2 Analysis of thermal Loading

Another important issue about the design consideration and requirements is the thermal loading issue and its effects on the designed supports. To explain briefly thermal loading becomes critical when a thermal gradient causes different elements of the microbalance to expand by different amounts. This differential expansion can be analyzed in terms of stress or of strain, equivalently. At some point, this stress can exceed the strength of the material, causing a crack to form and it will cause the supports structure to fail.

Failure due to the thermal instability can be prevented by increasing the material thermal conductivity, increasing its strength, decreasing its young modulus or increasing its toughness by crack tip blunting and crack deflection.

2.1.3 Mechanical Resistance

In design phase the electrodes are made of titanium, the three supports and the three springs are made of Ti-6Al-4V. Testing model is developed to realize supports and a clamp system, which are representative of the intended final geometry. Supports and springs will be used to realize a testing mockup and thus validate:

- Feasibility of the clamp system design
- Feasibility of the exciting, damping and measurement techniques based on the proposed idea.

2.2 TitaniumAlloy Ti-6Al-4V

The corrosion resistance of titanium is out of ordinary (almost as much as Platinum). It weighs 60% more than aluminum but with double resistance. It is as strong as steel but it weighs 45% less. Titanium alloys are generally classified into three main categories: alpha alloy, which contains neutral alloying elements (Sn) and/or Alpha stabilizers (Al,O) and are not heat treatable; Alpha + Beta alloys, which generally contains a combination of Alpha and Beta stabilizers and are heat treatable, and Beta Alloys, which are metastable and contain sufficient beta stabilizers (Mo,V) to completely retain beta phase upon quenching, and can be solution treated and aged to achieve significant increases in strength.

Ti-6Al-4V is known as the "workhorse" of the titanium industry because it is by far the most common Ti alloy, accounting for more than 50% of the total titanium usage. It is an Alpha + Beta alloys that is heat treatable to achieve moderate increase in strength.

Ti-6Al-4V offers a combination of high strength, light weight, formability and corrosion resistance, which have made it a world standard in aerospace applications.

Ti-6Al-4V may be considered in too many applications where a combination of high strength at low to moderate temperatures, lightweight and excellent corrosion resistance are required. Some of the many applications where this alloy has been used are aircraft engine turbine components, aircraft structural components, aerospace fasteners, high performance automotive parts, marine applications, medical devices and sport equipment.

The following table summarize the properties of Ti-6Al-4V.

Density[kg/m^3]	4428.8
Young Modulus[MPa]	110316
Poisson's Ratio	0.31
Ultimate Strength[MPa]	923.9
Yield Strength[MPa]	868.8
Thermal Expansion Coefficient [m/m°C]	$8.9 * 10^{-6}$
Thermal Conductivity[W/mK]	7.26

Table 1 Mechanical and Thermal Properties of Ti-6Al-4V

2.3 Supportsthicknesspreliminary design

The acceleration during the landing produces a force that has to be overcome by the microbalance supports. In case of having normal loads to the microbalance plane, the worst upcoming condition can be buckling phenomenon, while bending stress also arises for in-plane loading.
Both conditions will be analyzed in following paragraph, in order to find the minimum thickness of the microbalance supports.

2.3.1 Theory of Buckling

Experimental evidence has shown that for relatively long rods (slender) under compression load, occurs so called "Buckling" that is a phenomenon of collapse even when the stress applied is below the limit of resistance of the material.
If the physical length (L) of the rod is known and the compressive load has been set, then the design for buckling of a column reduces to three issues:

1. Settle on the end or boundary condition and determine its effective length L_{eff}.[44]
2. Determine the material, second moment of area product (EI) that is sufficient to prevent buckling
3. Insure that this cross section has sufficient area A so that the compressive stress is less than the allowable stress.

The easiest concept to grasp is that the design load P must be less than the critical buckling load P_{cr}. The critical buckling load is given by Euler's formula so:

$$P < P_{cr} = \frac{\pi^2 .\ EI}{L_{eff}^2} \qquad (2.1)$$

It is important to realize that the effective length of column is that which deflects into the shape of a half sine wave and that P_{cr} is not an actual load but a load-independent number that is a characteristic of a geometry and material of the column. It is important to define an appropriate safety factor FS for buckling (*usually greater than other safety factors*) that is given by the ratio between P and P_{cr}.

$$P \leq \frac{P_{cr}}{FS} = \frac{\pi^2 .\ EI}{FS\ .\ L_{eff}^2} \rightarrow\ I \geq \frac{P .\ FS\ .\ L_{eff}^2}{E\ .\ \pi^2} \qquad (2.2)$$

The expression on the right is the design equation where everything on its right-hand side is known or set for the time beings. FS is generally prescribed by a code or specification. Therefore, the left-hand side can be solved for I, which depends on the cross section geometry.

2.3.2 Buckling with an eccentric load

If the line of action of the resultant load P acting on the element does not coincide with the centroidal axis of the section, the beam is loaded eccentrically. figure (2-2)

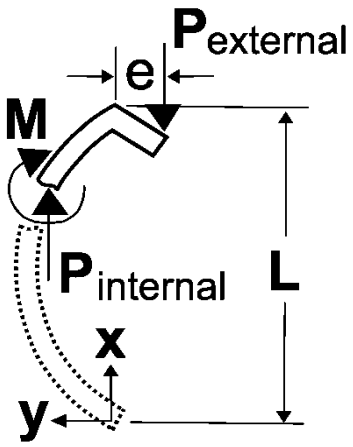

Figure 2-2 Eccentricity Loading and Buckling phenomena

The distance between the axis of the load and the axis of the column is the eccentricity e that generates a bending moment. The analytical formula that describes this situation is called Secant formula:

$$S = \frac{P}{A} = \frac{S_y}{1 + \left(\frac{ec}{k^2}\right).\sec\left[\left(\frac{L_{eff}}{2.k}\right).\sqrt{\frac{P}{AE}}\right]} \quad (2.3)$$

Where A is the cross section's Area of the support, S_y is the yield stress, E is the young modulus, ec is the eccentricity, $k^2 . A = I$. And I is the moment of inertia of the cross section.

2.3.3 Design Process

The load that may cause buckling is shown schematically in figure (2-3).

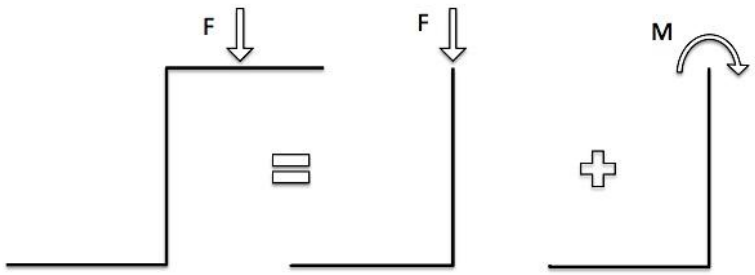

Figure 2-3 Load Condition of the Supports

The minimum thickness that springs and supports must have in order to avoid buckling can be calculated by iterating the "Secant formula" .
The iteration is performed using an iterative numerical method which minimize the following objective function:

$$f = P - \frac{A\,.\,S_y}{1 + \left(\frac{ec}{k^2}\right).\sec\left[\left(\frac{L_{eff}}{2.k}\right).\sqrt{\frac{P}{AE}}\right]} \quad (2.4)$$

The thickness of the elements is varied to find a minimum of f considering that at each iteration, load P has to be less than or at most equal to half of the critical load P_c. It should be mentioned that elastic support thickness determines both the loading P and the parameter k

Since the rod has a clamped-hinged constrained, the value of the effective length is $L_{eff} = 0.8.l$, figure (2-4).

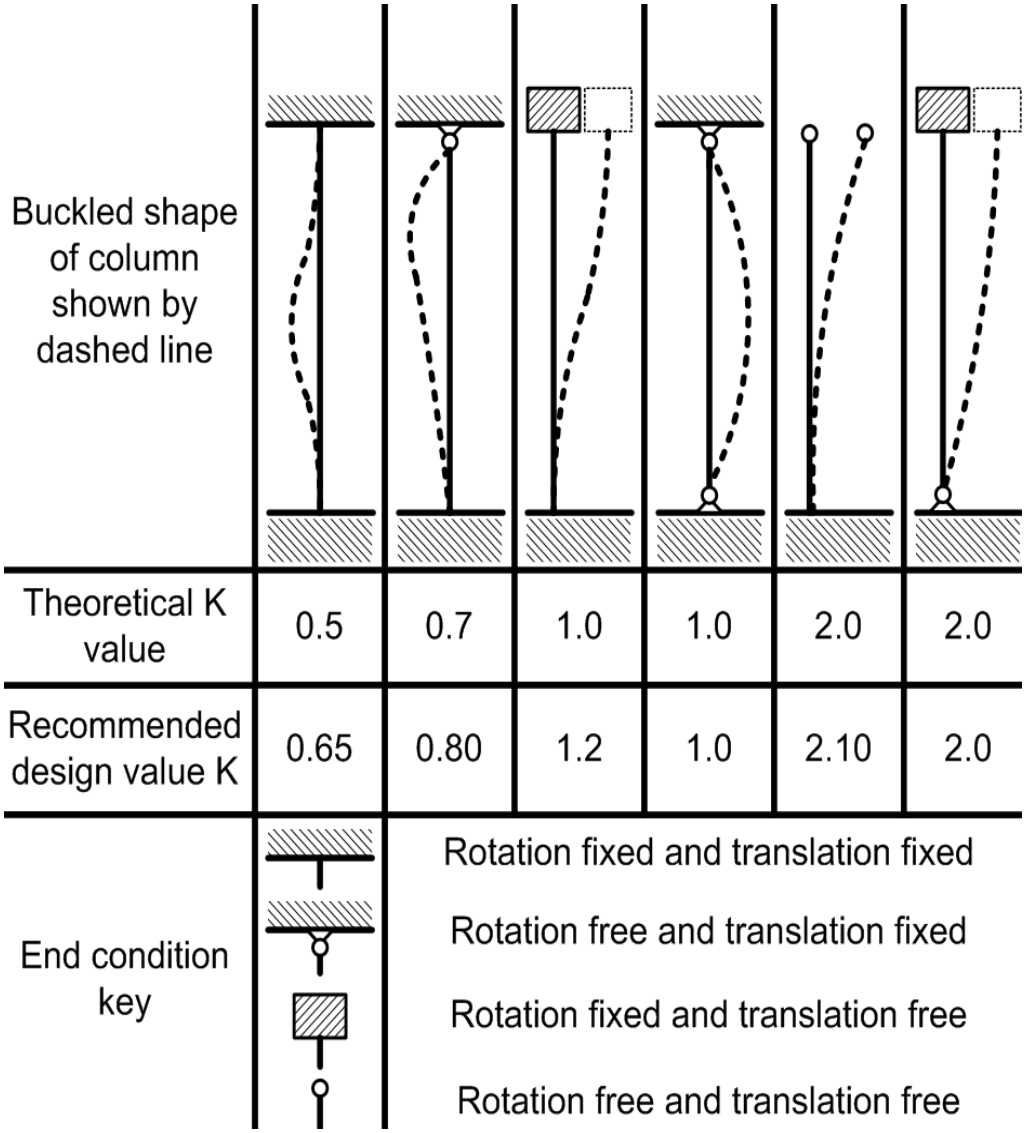

Figure 2-4 Value of effective Length depend on constraint type

At the end of the minimization, it is possible to check if the computed thickness is acceptable by comparing the yield stress with the maximum caused by eccentric loading:

$$\sigma_{max} = \frac{P}{A} + \frac{P \,.\, e}{\mathrm{W}.\left[1 - \left(\frac{P}{P_{cr}}\right)\right]} \quad (2.5)$$

Where W is the resistor modulus of the section and so far a rectangular section it is :

$$W = \frac{I}{\left(\frac{h}{2}\right)} = \frac{b.h^2}{(6)} \quad (2.6)$$

These calculations were done for the final model of the microbalance with the springs made of titanium alloy Ti-6Al-4V and also for the testing model of the microbalance.

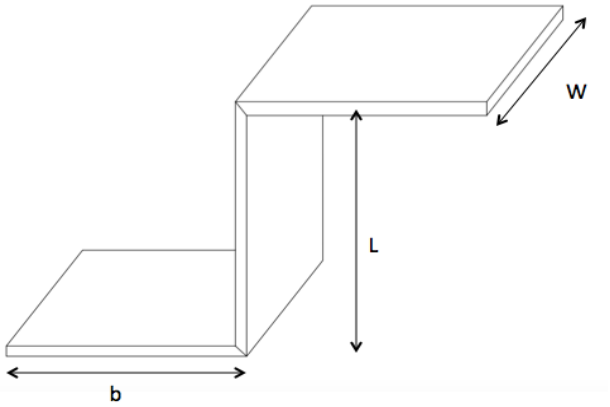

Figure 2-5 Dimensions of the Support

Lengthb [m]	$3 * 10^{-3}$
Widthw [m]	$3 * 10^{-3}$
Heightl [m]	$12 * 10^{-3}$
Thickness[m]	$0.1* 10^{-3}$

Table 2Dimension of the support

The force that could generates buckling is the one produced by the acceleration applied to the structure along the vertical axis . In this case all the three supports react at the same way, so the force that is applied at each of them can be computed as :

$$F = \frac{1}{3} . acceleration . \left(\frac{1}{3} Mass_{\ Quartz} + Mass_{\ Support\ +Spring}\right) (2.7)$$

Since the mass of the spring used to keep the quartz in a safe position (that is on the support) is unknown, during the design step , it is assumed that it's equal to half of the mass of the support, thus :

$$Mass_{\ Support\ +Spring} = Mass_{\ support} + Mass_{\ Spring} = \frac{3}{2} Mass_{\ support} \ (2.8)$$

2.3.4 Minimum thickness for bending moment

Since there is also a shear force that acts on the supports that produces a bending moment, it must be calculated the minimum thickness of the supports in order to stand.

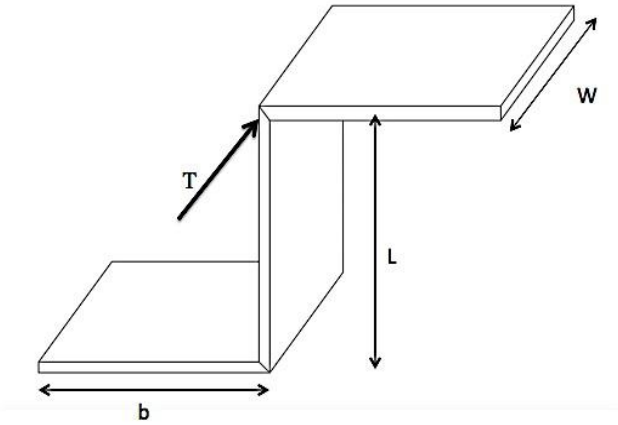

Figure 2-6 Shear Force acting on the Support

The three supports are positioned 120° relative with respect to each other. Figure (2-7)

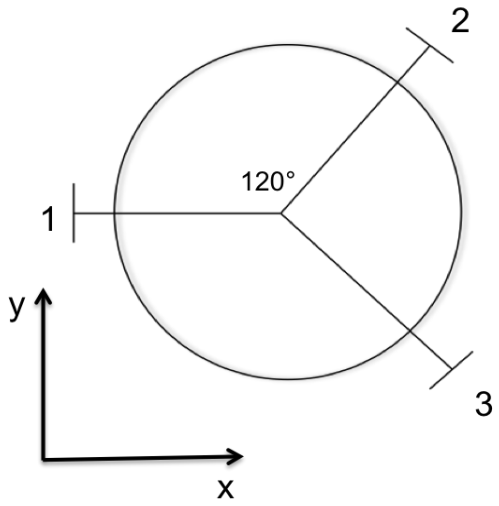

Figure 2-7 Position of the Three supports

This configuration allows a thermally compliant mounting, by properly design radial elastic support stiffness, so that stresses due to variation in temperature are reduced.

By the way a shear force T is generated when the acceleration is applied along the x-axis or y-axis. Considering the acceleration applied along the y-direction, all the three supports counteract the force. If the acceleration is applied along the x-direction, the support number 1 is yielding in this direction, so only supports number 2 and 3 must match the global force.

Since we should always consider the most critical condition, the case in which the acceleration is applied along the x-axis must be considered. By a simple calculation it is obvious that the discussed shear force is:

$$F = \frac{1}{\sqrt{3}} . acceleration . \left(\frac{1}{3} Mass_{\ Quartz} + Mass_{\ Support\ +Spring}\right) \quad (2.9)$$

That produces a torque on the support equal to:

$$M_f = T . l \quad (2.10)$$

Considering a safety factor equal to $sf = 1.5$ the torque acting on each support is

$$M_{\ tot} = M_f . Sf \quad (2.11)$$

so the stress produces on the support by the bending moment is:

$$\sigma_{\ max} = \frac{M_{\ tot}}{W} \quad (2.12)$$

Where W is the resistor modulus of the section.

2.3.5 Results of the final model of microbalance

Mechanical properties of Ti-6Al-4V useful for the calculations :

$\sigma_{max} = \sigma_y$	$8.68 * 10^{8}$[Pa]
Young Modulus	$1.1 * 10^{11}$[Pa]
Density	4428.78[kg/m^3]

The maximum stress that the structure can withstand is the yield stress.

The mechanical properties and dimensions of the quartz useful for the calculations are:

Thickness of Quartz	0.160[mm]
QuartzDiameter	13.95[mm]
Density	2200[kg/m^3]

It is now possible to calculate the mass of the quartz and the mass of the supports considering *h=0.1 mm* . (thickness of the supports)

Mass of the Quartz	$5.38 * 10^{-4}$[kg]
Mass of the Support	$2.26 * 10^{-5}$[kg]
Compressive load on each support	10^{-1}[N]

2.4 Design of the Clampingsystem

The clamp system is composed by three springs positioned in correspondence of the supports in order to secure the microbalance.
The three springs must be designed in order to avoid the movement of the microbalance under the force produced by the acceleration.

Figure (2-8) shows how elastic supports and the clamps are positioned. The minimum force (N) that each spring must produce in order to avoid the movement of the microbalance must be equal to the force generated by the acceleration (a=50.g=490.5 $\frac{m}{s^2}$) applied to the microbalance. It is possible to calculate the minimum force knowing the static friction coefficient between the spring and microbalance (μ_s).

$$M_{micro} = M_{Quartz}$$
$$F = M_{micro} \cdot a$$
$$N \cdot \mu_s \geq M_{microbalance} \cdot a \qquad (2.13)$$

Where (N) is the normal force that the spring must generate, μ_s is the static friction coefficient between the microbalance and the spring, a is the acceleration applied to the microbalance and M_{micro} is the mass of the quartz plus the mass of the support plus the mass of the spring which can be approximated as half of the mass of the support.

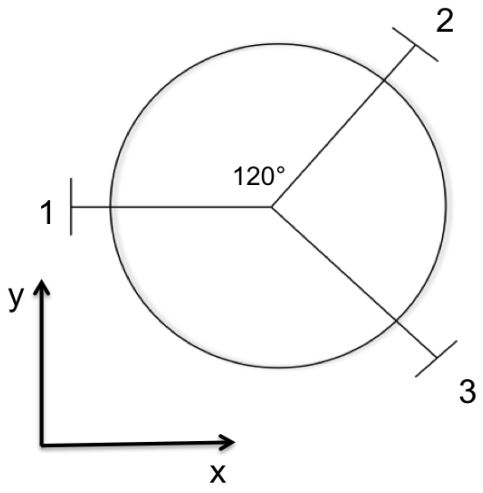

Figure 2-8 Position of the Supports

Thus in order to prevent the sliding of the sensor, it is necessary to design the supports in a way that they apply required force F, which is coming out from the multiplication of mass of the quartz (M_{quartz}) into the acceleration (50g). This force is, which is equally distributed over three supports is provided as a pre-load by changing the geometry and shape of the support. Considering the height of the C-shaped stand, we choose 12 mm for the length of the final model of the S-shaped support with a curve on the topside handle.

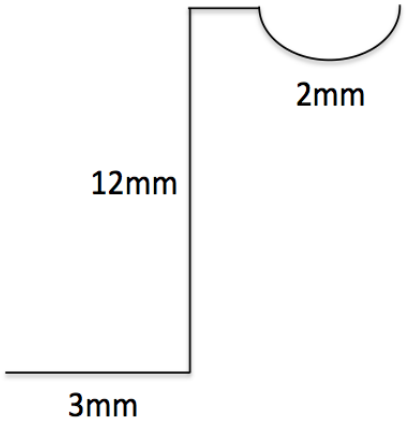

Figure 2-9 Dimensions of S-shaped support

Considering the acceleration applied along the y direction (figure 2-9) , all the three springs counteract the load, if the acceleration is applied along the x direction, the support number 2 is yielding in this direction so the global force must be matched only by 1st and 3rd spring. This is true if stiffness of the support in radial direction is negligible with respect to transversal and axial ones, same as actual design, where supports have to provide a thermally compliant mounting to avoid stresses arising from temperature variation.
Figure (2-10) shows how the force is decomposed tangentially to the two supports that react.

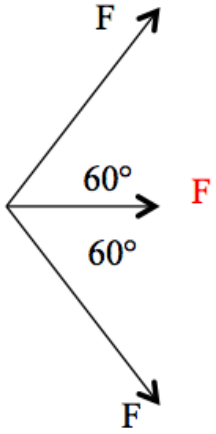

Figure 2-10 Decomposition of the Force

It is obvious that each of the two springs must counteract a force equal to F [N]. The following table shows the results of calculations carried out for the final model of the microbalance.

Results for the final model of the Microbalance	
Minimum Force that must be generated to keep the Quartz [N]	$8.8 *10^{-2}$
Compressive Load Applied on Each support on contact Area [N]	$1.05 *10^{-1}$
Critical Buckling Load considered for the supports [N]	2.95
Safety Factor for buckling phenomenon usually greater than other safety Factors	28
Moment of Area of the Cross section of the support [m^4]	$2.5 *10^{-16}$
Generated Shear Force [N]	$5.2*10^{-2}$
Maximum allowable bending Stress generated by shear force [Pa]	$6.3*10^{6}$
Mass of the support [kg]	$2.4 *10^{-5}$
Mass of the Quartz [kg]	$5.4 *10^{-4}$
Thickness of the support [m]	$1.5 * 10^{-4}$
Static Friction Coefficient between Ti-quartz	$3.6 *10^{-1}$

Table 3 Results of the final model of the microbalance

2.4.1 Contact Pressure

The Hertz theory shows the determination of stresses and deformations that are produced by pressing one against the other two elastic curve bodies. It is assumed that:

- Perfect elastic materials
- Absence of frictional force
- Contact surface smaller than the size of the bodies in contact

As it is shown in figure (2-11), the contact is not on a point , but on an area of finite dimensions. Considering the case of contact between two cylinders or between a cylinder and a plane, maximum pressure can be calculated as following:

$$F = \frac{1}{2}\,\pi\,.\,a\,.\,L\,.\,p_{max} \qquad (2.14)$$

$$p_{med} = \frac{F}{Area} = \frac{F}{2aL} \qquad (2.15)$$

$$p_{max} = \frac{4}{\pi}\,.\,p_{med} \qquad (2.16)$$

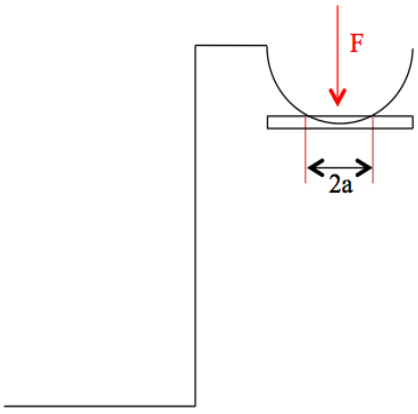

Figure 2-11 Contact Area

The contact area is defined as :

$$a = \sqrt{\left(\frac{2}{\pi}.\frac{m_1 + m_2}{B}.\frac{F}{L}\right)} \qquad (2.17)$$

where :

$$m_1 = \frac{1 - \nu_1^2}{E_1} \qquad (2.18)$$

$$m_2 = \frac{1 - \nu_2^2}{E_1} \qquad (2.19)$$

$$B = \frac{1}{2}\left(\frac{1}{R_1} + \frac{1}{R_2}\right) (2.20)$$

$\nu_1$andν_2 are the posson ratio, E_1 and E_2 are the young modulus, R_1 and R_2 are the radius of the two cylinders. In case of contact between a cylinder and a plane $R_2 = \infty$, So for the case of contact between a cylinder and a plane surface:

$$a = \sqrt{\left(\frac{4}{\pi}.R_1(m_1 + m_2).\frac{F}{L}\right)} (2.21)$$

The maximum pressure that the quartz can withstand is equal to its ultimate strength (50MPa), the safety coefficient $sf = 3$, F is the force that must be produced in order to prevent the movement of the quartz when the acceleration of $490.5\frac{m}{s^2}$ is applied.

Using the Hertzian contact theory, it is possible to calculate the minimum contact area that avoids the failure of the quartz crystal.
The following table show the results for the final model of the microbalance.

Ti-6Al-4V	
R	0.001[m]
F	0.9[N]
L	0.0015[m]
P_{max}	$1.6 *10^{8}$[Pa]
M_1	$8.19*10^{-12}$
M_2	$1.35*10^{-11}$
ν_1	$3.1*10^{-1}$
ν_2	$1.7*10^{-1}$
E	$1.1*10^{11}$[Pa]
E_q	$7.7*10^{10}$[Pa]
sf	3
$P_{maxFinal}$	$1.67*10^{8}$[Pa]
a	$1.3*10^{-6}$[m/s^2]
Area	$7.65*10^{-9}$[m^2]

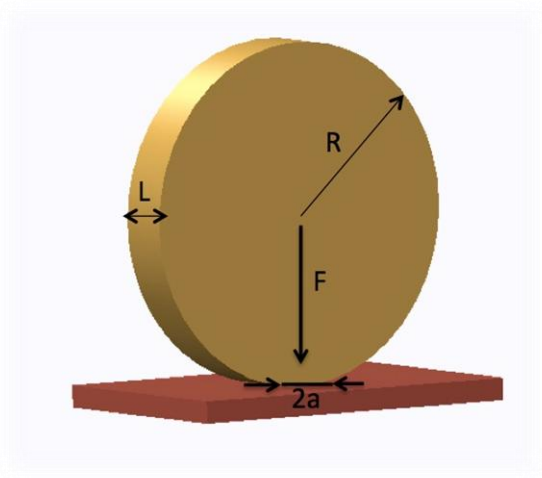

Figure 2-12 Contact Surface

2.5 Design of the springs

The characteristic curve of a spring is generally defined as a function of a external force, P, and the displacement of the point of application of the load, the arrow f.

$$P = P(f)$$

The stiffness of the support is defined as :

$$k = \frac{dP}{df} \qquad (2.22)$$

In this case the spring is a linear spring thus the stiffness k is constant, in particular the designed spring is a flexural spring. Figure (2-13)

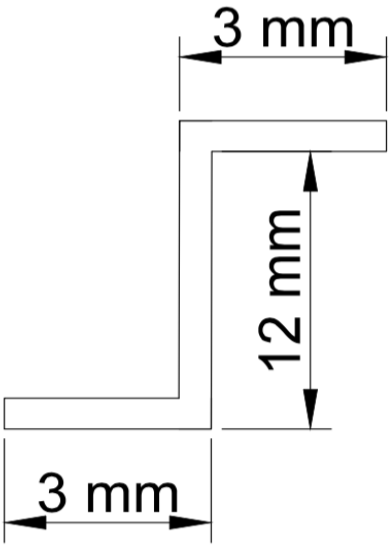

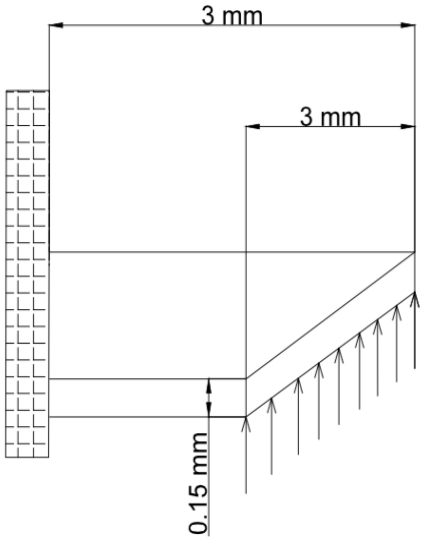

Figure 2-13 Stand Dimension Figure 2-14 Model o f Flexural Loading

$$K = \frac{3EI}{L^3} \qquad (2.23)$$

The mentioned term *" I "* is calculated with respect to the axis, which passes trough the centroid of the cross section and is perpendicular to the applied load. Deflection δ is calculated as:

$$\delta = \frac{PL}{AE} \quad \rightarrow K = \frac{P}{\delta} = \frac{AE}{L} \qquad (2.24)$$

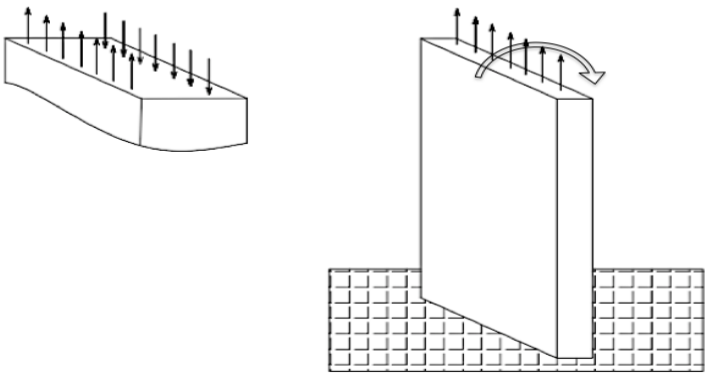

Figure 2-15 Model of column

As it is explained before, the three springs must exert a force on the crystal in order to prevent its movement. It is necessary to calculate their minimum stiffness (K_{min}) to ensure the proper function of the springs. The minimum stiffness of the springs must be such that :

$$F_{min} = K_{min} * \Delta l$$

where F_{min} is the minimum force that must be exerted, K_{min} is the minimum stiffness that the spring must have in order to generate a force equal to F_{min} when they are elongated of Δl. (That is equal to the thickness of the crystal).

Another important factor that must be considered during the design of the springs is the temperature in the mounting location.

The spring is mounted at temperature of 20 °C, while the working temperature is about -200 to 150 °C. Thus there exist a constant variation of elongation between the quartz and spring. To calculate the elongation of the crystal and also of the spring, it is used following formula:

$$L_{fin} = L_{in} + (1 + \lambda \Delta t)$$

And it is evaluated that the difference between the two elongations was so small so it can be negligible in design of the springs.

In order to prevent the sliding of the quartz minimum force that springs must exert is 0.09 N. The thickness of the quartz crystal is 0.16 mm, so when the springs will be mounted on the supports there will be an elongation Δl of the spring equal to the thickness of the quartz. The analytical results of the stiffness are shown in following table.

b[mm]	3
Thickness [mm]	0.15
L_{total}[mm]	12
E [Mpa]	110316
I [mm^4]	0.0025
K [N/m]	558
F [N]	1
Δl [mm]	0.16
Density [kg/m^3]	4428.78
Width [mm]	3

Table 4 Table of results

By creating the FEM model the evaluated analytical stiffness is verified. In order to simulate the spring and calculating the stiffness we applied a load equal to 1N along x , y and z directions, and the evaluated deformation with respect to each axis were calculated as the stiffness with respect to each axis.

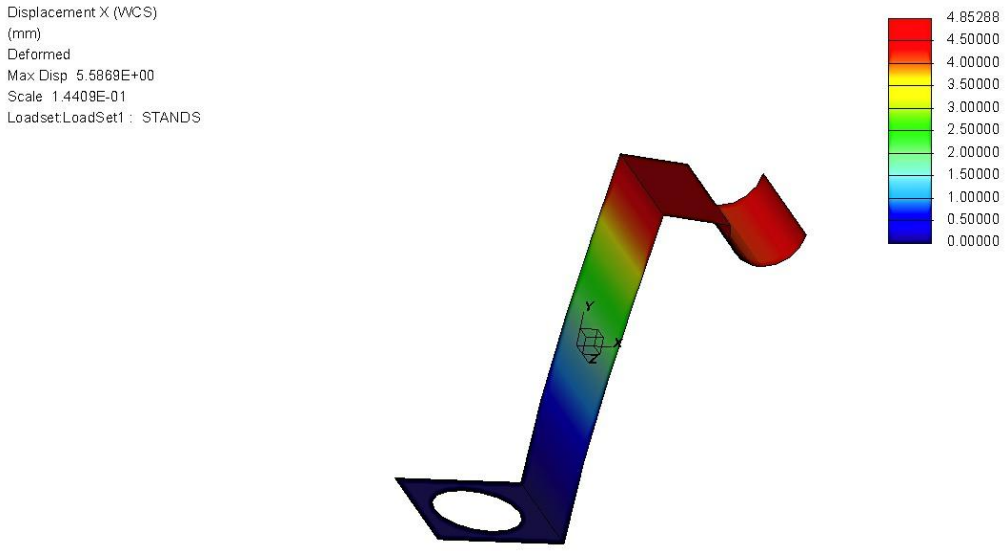

Figure 2-16 Displacement in x direction

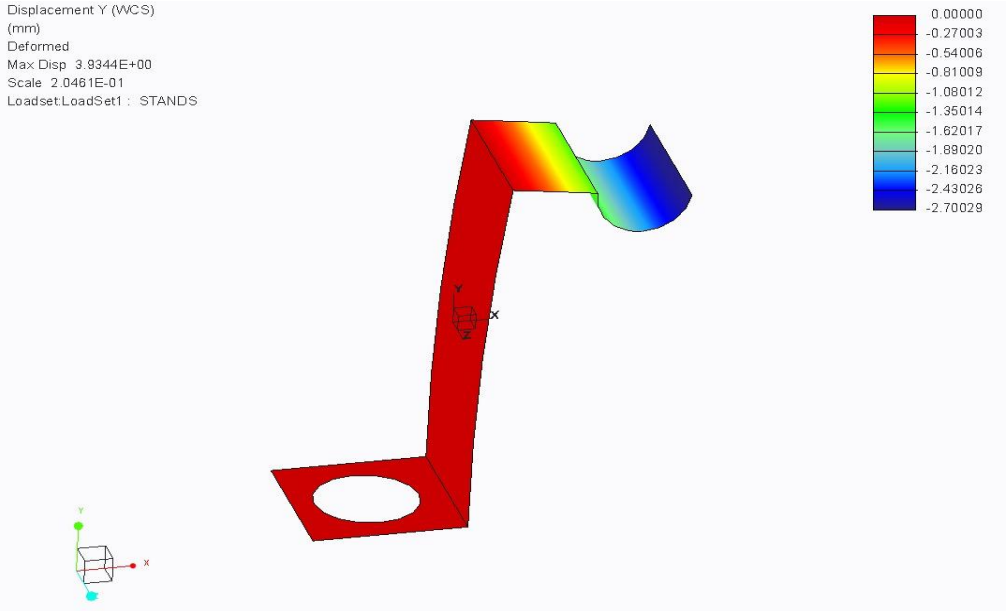

Figure 2-17 Displacement in y Direction (mm)

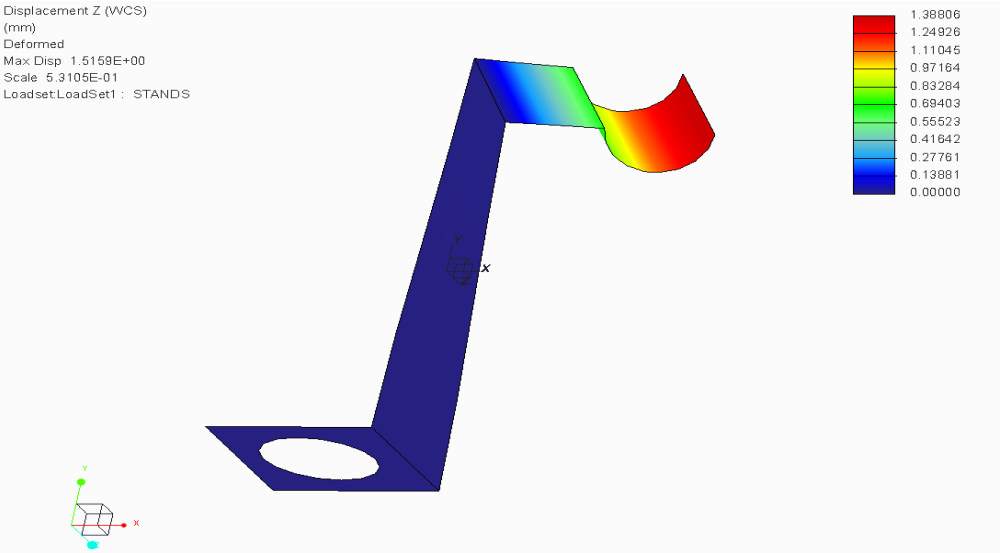

Figure 2-18 Displacement in z Direction (mm)

Having these values, the stiffness of the spring can be calculated with respect to each axis as:$F = k * \Delta l$

Result of evaluated Stiffness K [N/m]	
Kx	178
Ky	254.5
Kz	662.3

Table 5 Table of Results

2.6 Microbalance FEM model – Feasibility of QCM Configuration

This section describes the mechanical analysis performed within the framework of the CAM project in order to compare different building solutions and assess feasibility of the baseline QCM configuration.Beside usage of titanium supports, aluminum material has been used as well. This is because the thermal design of the CAM project was under development and final configuration was not achieved.

In order to model the behavior of the QCM and verify the mechanical resistance against expected loading a finite element model is developed base on CREO 2.0 PTC software. The model consists of three insulating supports and the crystal. Mechanical properties of the material are provided in table 7.

Material	*Elastic modulus [MPa]*	*Density [Kg/m^3]*	*Poisson Ratio*	*CTE [1/°C]*	*Thermal conductivity [W/m °C]*
Quartz crystal*	From 76500 to 97200	2649	0.17	From 7.1 to 13.2 10^{-6}	From 6.2to 10.7
Ti 6Al 4V	113800	4430	0.342	8.6 10^{-6}	6.7
Al 7075 T6	71700	2810	0.33	25.2 10^{-6}	130

Table 6 Supports mechanical properties, Quartz crystal properties can be found in[45]

*To account for the crystal anisotropy worst case value has been assumed independently of the actual axis.

It is obvious that the quartz crystal has different elastic modules, thermal conductivities and CTEs depending on the crystal axis direction. For these preliminary and mainly comparative analyses the following worst cases have been adopted.

- Thermo-elastic analysis (with titanium supports), Quartz crystal and elastic modules set to $13.2 * 10^{-6}$ 1/°C and 97200 MPa respectively.
- Thermo-elastic analysis, Aluminum supports, Quartz crystal and elastic modules set to $7.1 * 10^{-6}$ 1/°C and 97200 MPa.
- Modal analysis with both support material and quartz elastic moduls set to 76500 Mpa.

Modifying the support's geometry i.e. width, height and the thickness performs preliminary mechanical design of the supports. The design is driven by:

- Mechanical resistance against 500 m/s^2 quasi static loading. The loading takes into account the expected forcing due to the sweep sine (20g) and random excitation (PSD spectrum with 20g RMS) as for reference.
- Dynamic behaviour with first natural frequency larger than 1000 Hz.
- Thermo-elastic stress minimization.

Among different requirements, the most critical one is expected to be thermo-elastic stress, cause the crystal shall withstand minimum temperature of -200°C and maximum of 150°C. More over as shown by the preliminary thermal design huge temperature difference is expected for some configuration during the regeneration phases. Thus difference cases have been analyzed.

- Mounting at ambient temperature (25°C) and cooling to -200°C.
- Regeneration from -120°C to 200 °C.
- Regeneration from -200°C to 100°C.

Two different contact shapes have been analyzed, i.e. cylindrical and spherical type and preliminary size of the support is summarized hereafter.

Parameter	Width	Length	Thickness	Contact radius
Value	3 mm	7-12 mm	0.15 mm	1 mm

Table 7 Parameters and Values

The cylindrical and spherical contact shapes provided maximum pressure of 71 MPa and 35 MPa, respectively. Thus, the maximum pressure resistance is expected to be well within the limits even with changes that might be needed in the detailed design phase. Actual contact areas are about 0.01 mm^2.

2.6.1 Thermo-elastic Analysis

From now on the results of the thermo elastic analysis is provided.

Mounting:

The following figures provide the results of the thermo-elastic analysis due to the mounting at 25°C and cooling down to -200°C. Figure (2.19) and Figure (2-20) show thermo-elastic stresses resulting from the mounting with rectangular contact area.

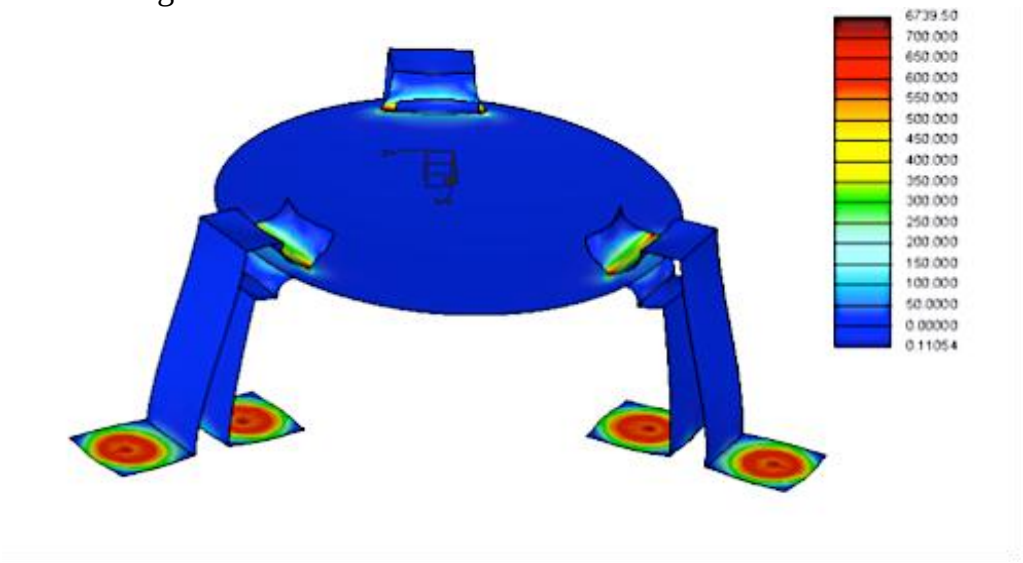

Figure 2-19 Thermo-elastic stress on Microbalance, supports and Rectangular area

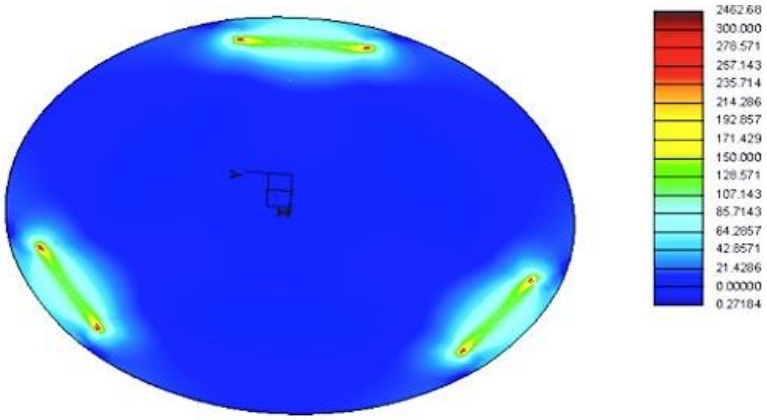

Figure 2-20 Thermo elastic stress on Microbalance, supports and Rectangular area

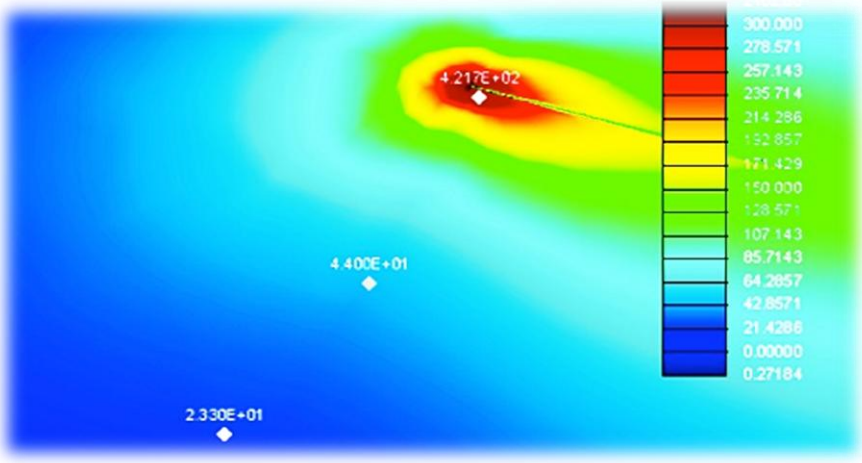

Figure 2-21 Thermo-elastic stress on Microbalance and Rectangular area

Deformed configuration and related thermo-elastic stresses are shown in following figures. The contact area was in circular shape.

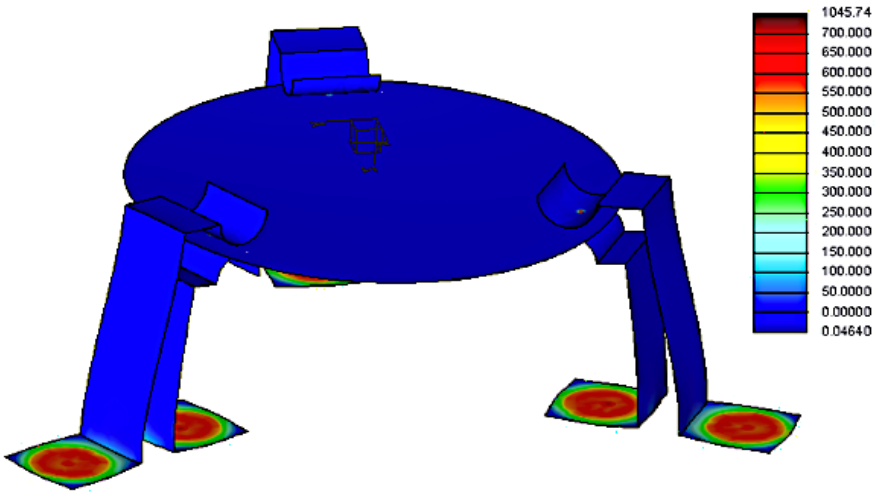

Figure 2-22 Thermo elastic stress on Microbalance, Circular contact area/Aluminum supports

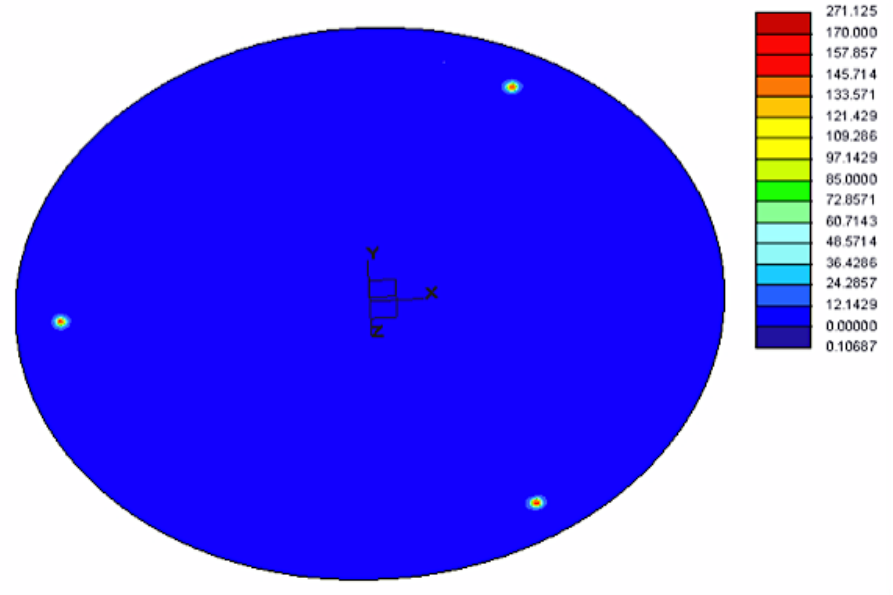

Figure 2-23 Thermo-elastic stress on Microbalance, Aluminum supports , Circular contact Area

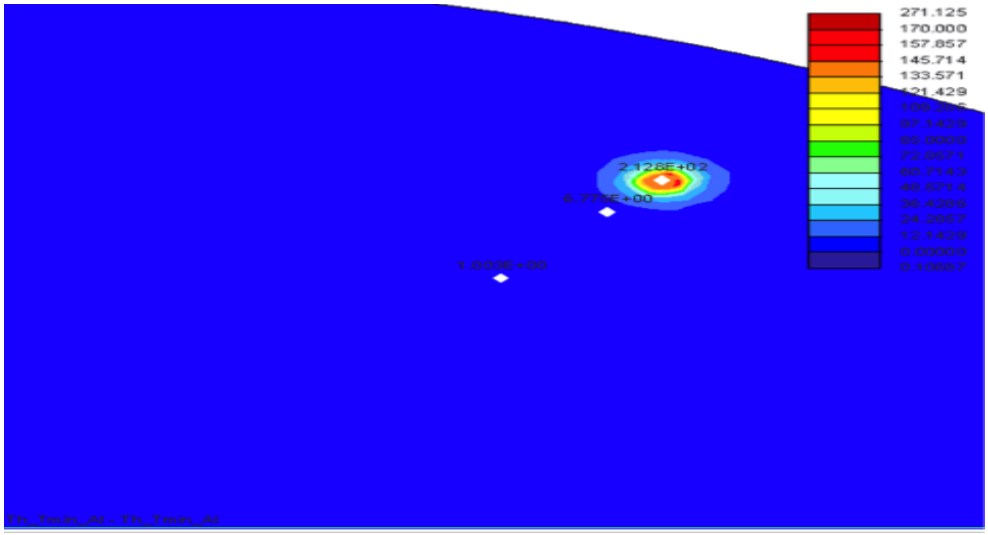

Figure 2-24Thermo-elastic stress on Crystal, Circular area and aluminum supports

Comparison between the mounting configurations shows that the circular contact areas reduce the thermo-elastic stresses. Thus, the circular area is considered as a baseline for dynamic and quasi-static analysis.

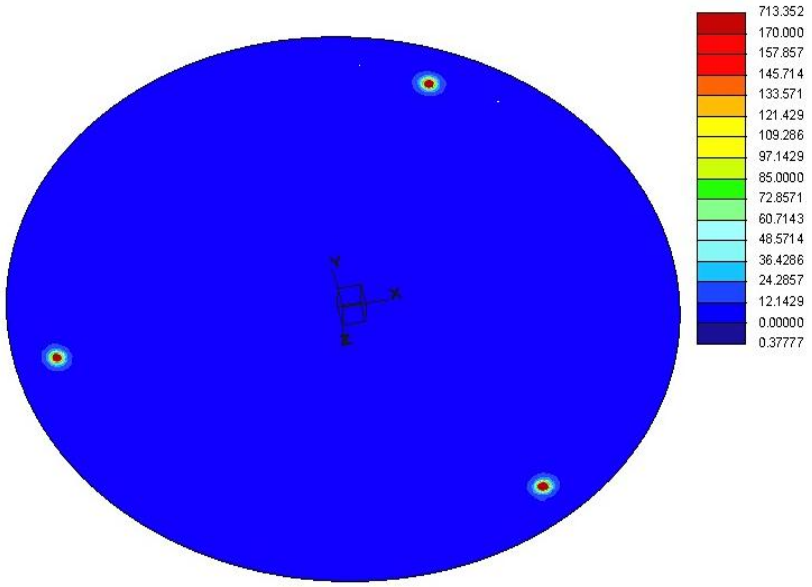

Figure 2-25Thermo-elastic stress on Crystal, Circular area and aluminum supports

By the way both configurations (and materials) show that high stresses are generated in contact regions. However these are mostly result of bending generated by the links in the contact regions but are not expected to see in practical condition while the spherical contact is free to rotate. In fact, the rigid link situated in the model does not allow the rotation between the cylindrical/spherical extremity of the supports and the crystal.

But this is only an effective way to represent the link without going in non-linear calculations with gap elements. Therefore calculated results in the region near the connections are overestimated and should not be considered.
The Von-Misses stresses over the crystal reduce of two orders of magnitude out of the contact areas, up to the crystal center. In these regions, computed stresses are in range of 2-15 MPa, leading to positive modulus, i.e. from 0.8 to 13.

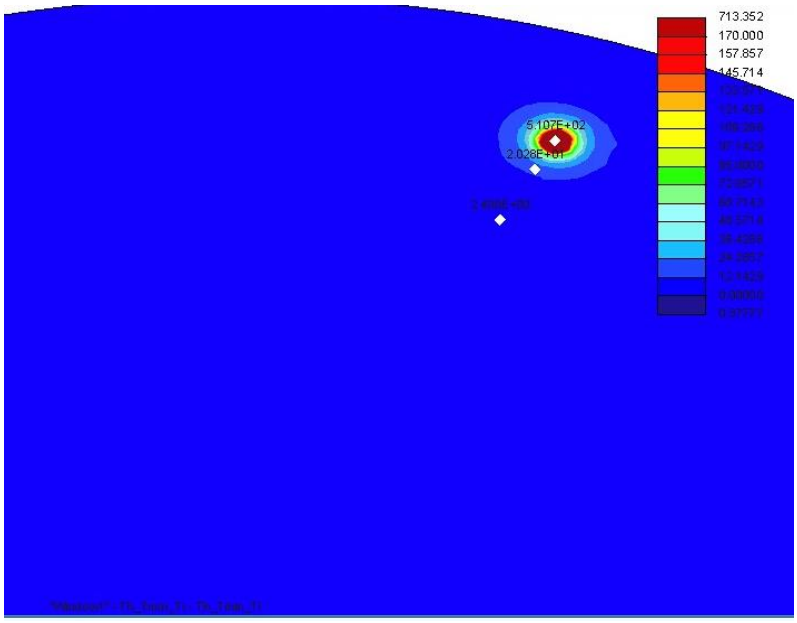

Figure 2-26 Thermo elastic stress on Crystals, Circular area/ Titanium supports

2.6.2 Regeneration to 200°C from -120°C

In order to simulate regeneration at 200 °C, temperature distribution (Cold case A) computed with the thermal model has been applied to the QCM assembly. The following figure shows the applied temperature field. Because of the thermo-elastic stress due to the mounting, the following analyses have been performed assuming circular contact area between the supports and the crystal.

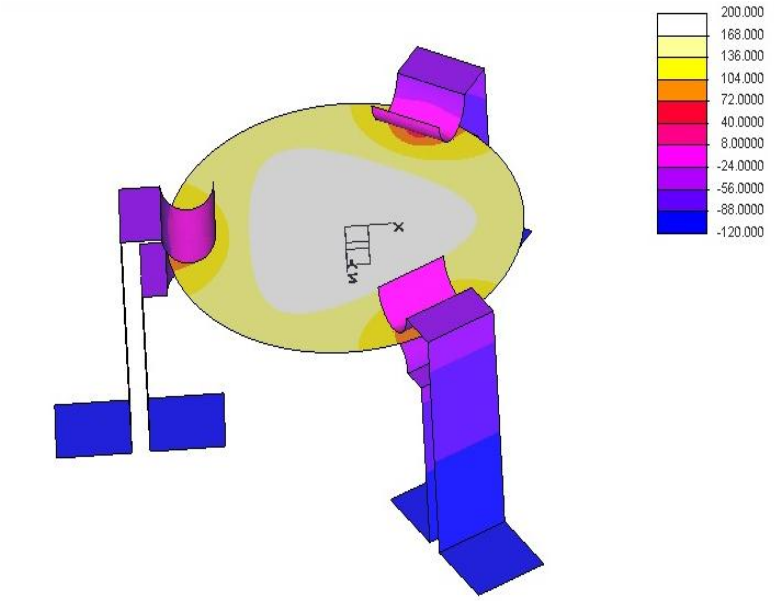

Figure 2-27 Temperature distribution cold case A, Aluminum supports, regeneration at 200°

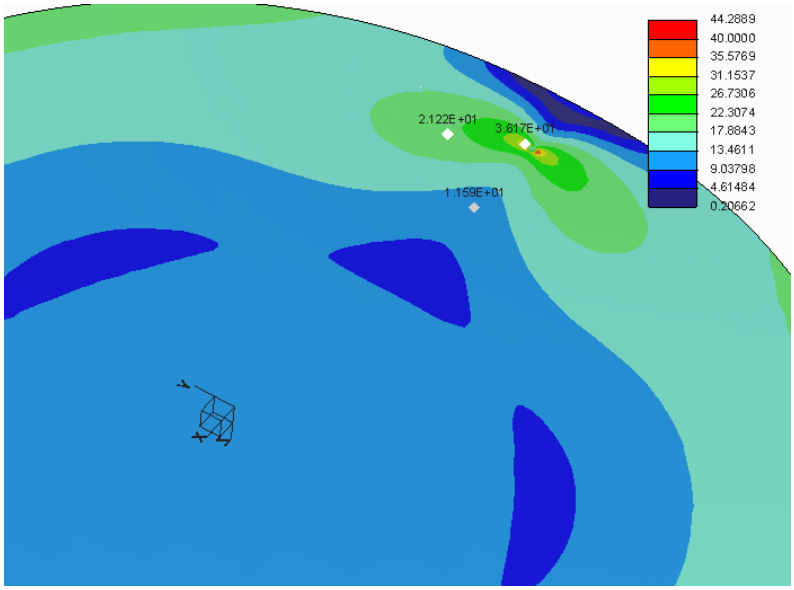

Figure 2-28 Thermoelastic stress due to the regeneration, Aluminum supports

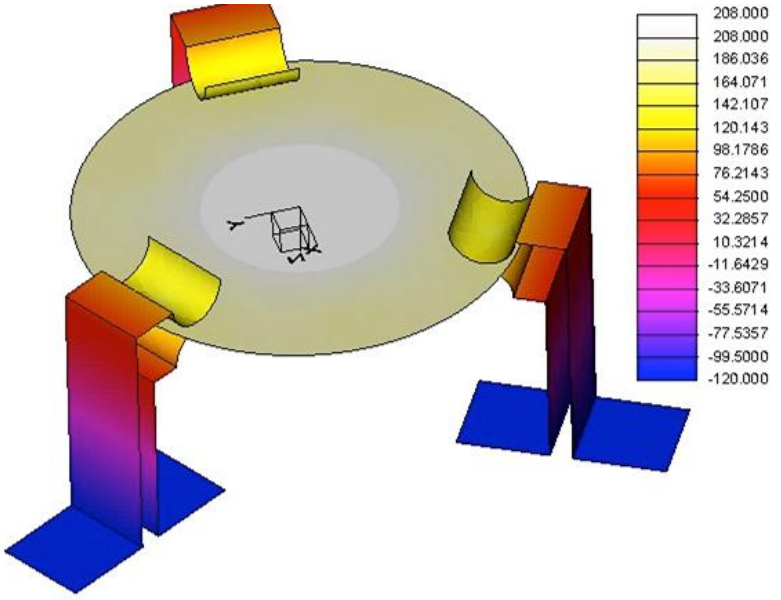

Figure 2-29 Temperature Distribution Cold case A, titanium supports, regeneration at 200°C

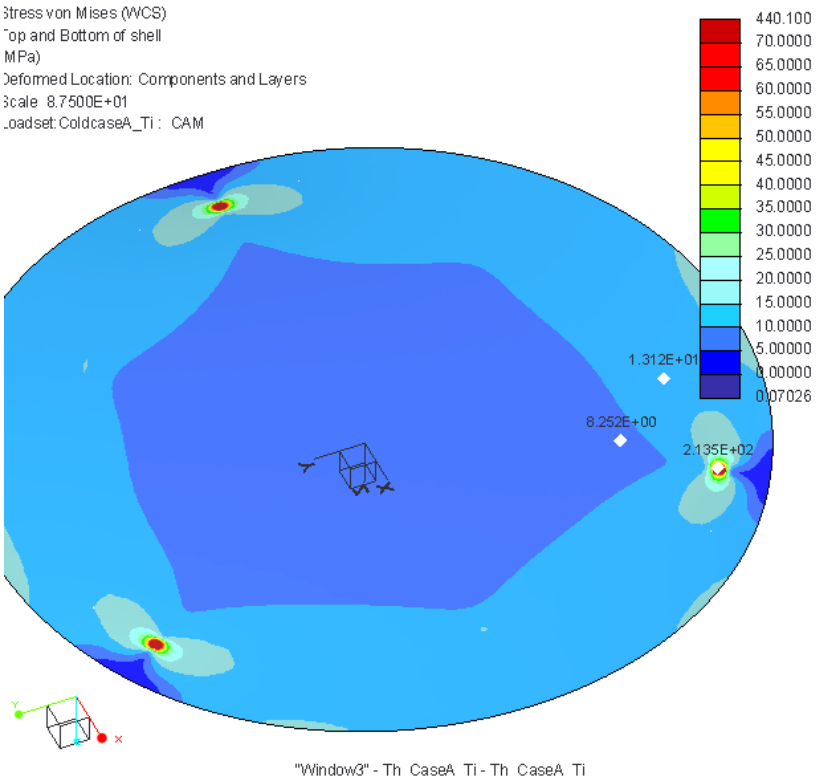

Figure 2-30 Thermo-elastic stress due to the regeneration, Titanium.

In case of aluminum supports, the maximum Von-Misses stress, about 44 MPa, is located at the connection point between crystal and the support. As it is calculated by previous analysis, larger stress is expected due to the CTE mismatch between crystal and the supports as a result of merge type constraint between linked surfaces.
In the region where the effect of the connections is not present, the Von-Misses stress ranges between 17 and 6 MPa. The result allows achieving MOS for the worst case at 0.61.
In the case of titanium supports, the maximum Von-Misses stress is about 440 MPa, is located at the connections between the crystal and the support. As for the above analysis, this result has to be discarded since due to a not representative connection between the crystal and the quartz. In the other areas the computed Von-Misses stresses vary between 13 and 8.6 MPa, leading to minimum modulus of about 1.1.

2.6.3 Regeneration to 100°C from -200°C

In order to simulate regeneration at 100 °C, temperature distribution (Cold case B) computed with the thermal model has been applied to the QCM assembly. The following figure shows the applied temperature.

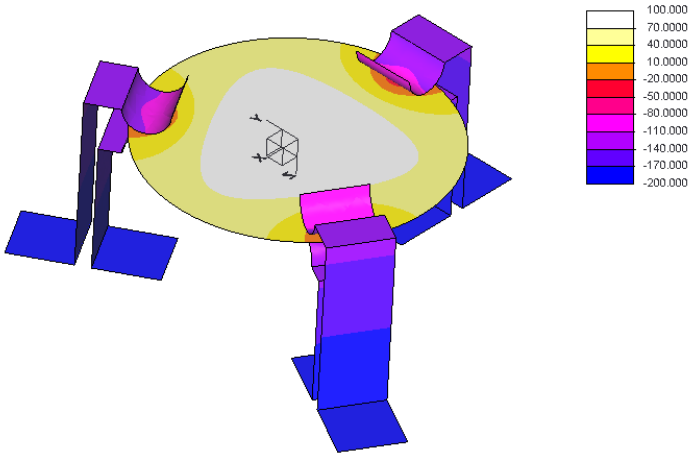

Figure 2-31 Temperature distribution Cold case B, Regeneration at 100°C

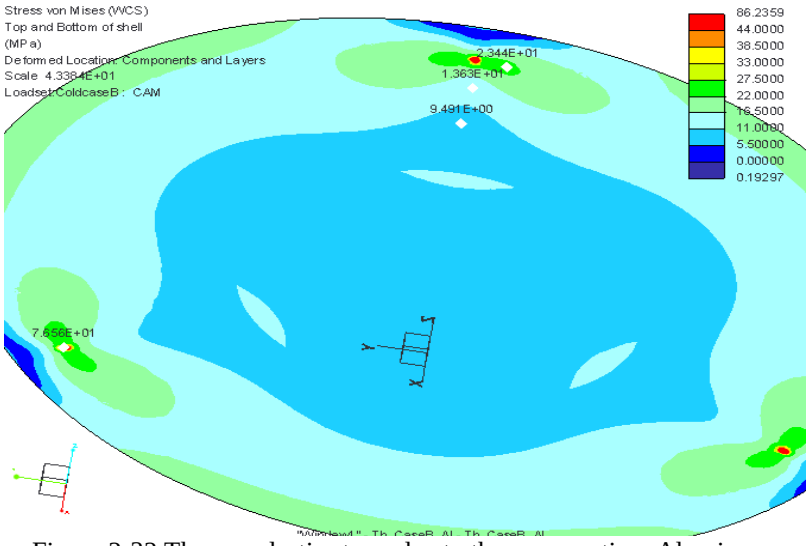

Figure 2-32 Thermo-elastic stress due to the regeneration, Aluminum

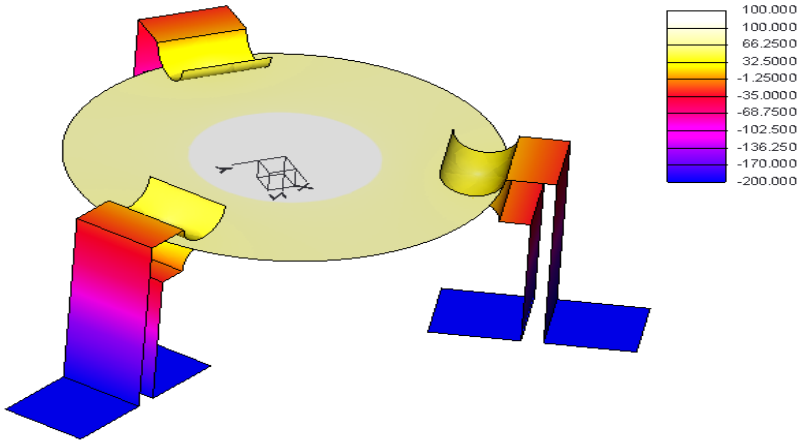

Figure 2-33 Temperature Distribution Cold case B , Titanium supports, regeneration at 100 °C

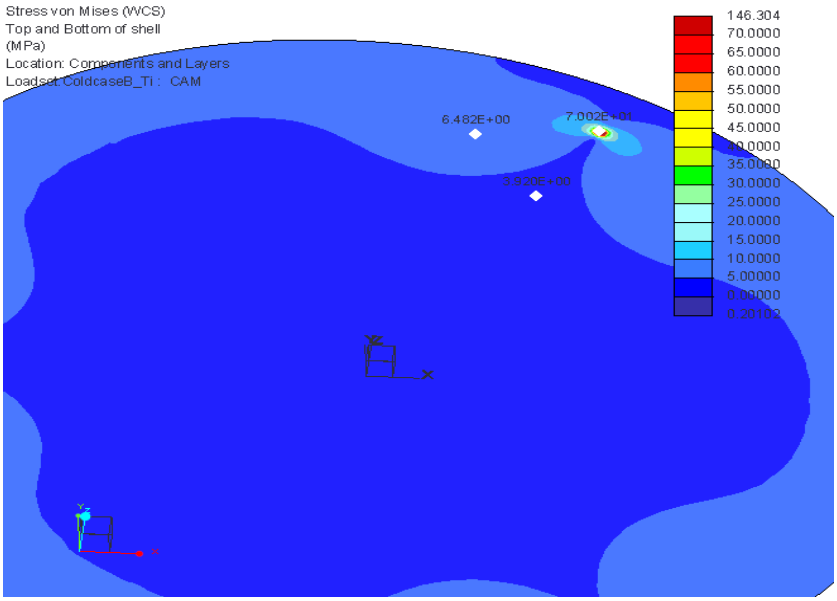

Figure 2-34 Thermo-elastic stress due to the regeneration, Titanium

As for the regeneration at 200°C, the result shows that the maximum stress in case of aluminum supports (about 86 MPa) is reached in the region where crystal and supports are connected. As demonstrated above, that area should be discarded since it does not represent the actual constraint conditions.

The Von-Misses stress distribution is similar to the one obtained in the previous case and provides a maximum set to about 13.6 MPa. The result leads to an acceptable modulus, i.e. 1.01.
Similar results are obtained with titanium supports analysis that showsmaximum Von-Misses stress of about 8.5 MPa in the region where the effect added by connection is not present.
The maximum stress over the aluminum support is located at the constraints. Von-Misses stress exceeds the yielding limit there. This result is not representative of the true stress condition since the deformation due to the temperature change is not allowed by the constraint. The worst-true case would be located at the position where bending of the supports is present. The computed stress is about 170 MPa, leading to a modulus equal to 0.97.

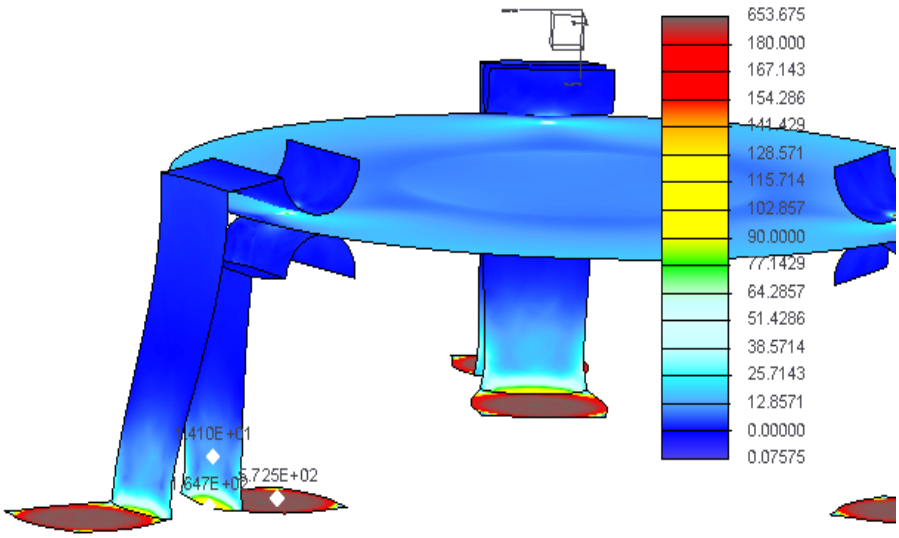

Figure 2-35 Von-Misses Stress on Aluminum supports

Similar result is achieved in the case of titanium supports, with maximum Von-Misses stress set to about 50 MPa, providing a modulus of about 10.

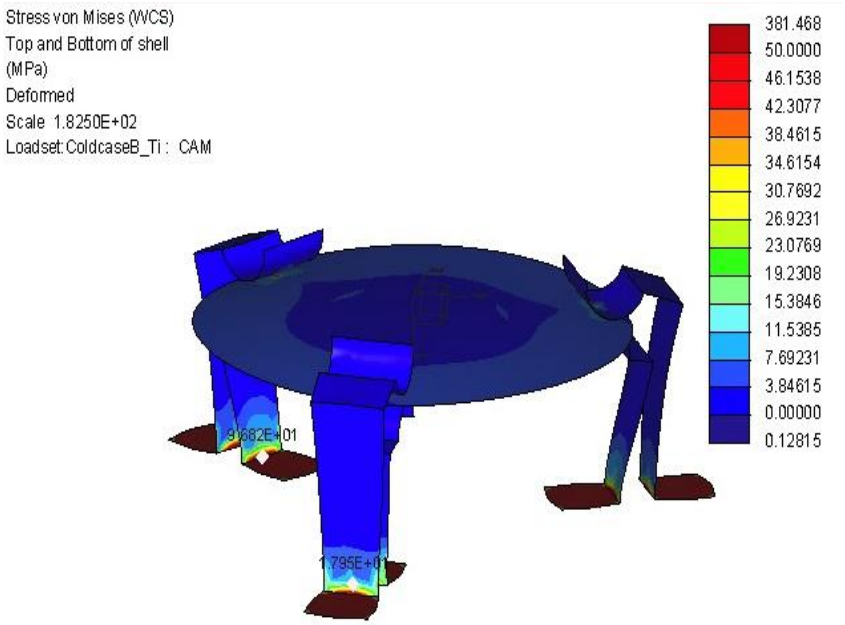

Figure 2-36 Von Misses Stress on Aluminum Supports

2.6.4 Modal Analysis

Modal analysis is performed to assess the microbalance dynamic behavior. The model with circular contact area is used varying the support's material. Supports have been constrained along a circumference with 2 mm diameter. The following table provides the first three modes computed using supports made with titanium and aluminum alloys. Computed modes are above the frequency range, where the expected random excitation has its maximum amplitude (200 m/s^2 RMS acceleration value).

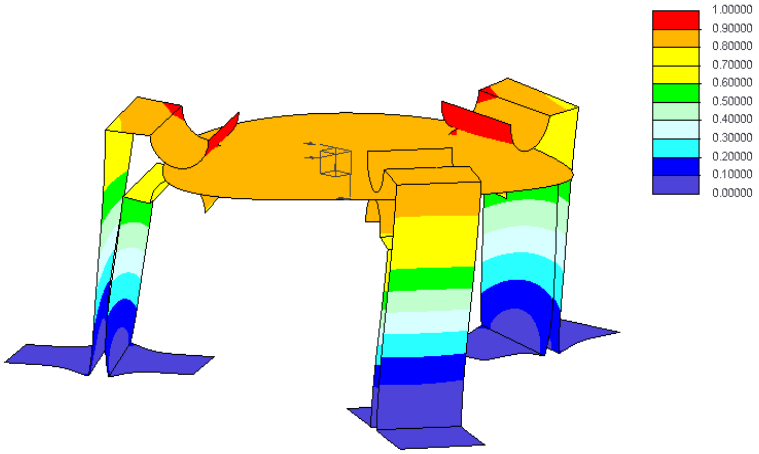

Figure 2-37 QCM 1st vibration mode

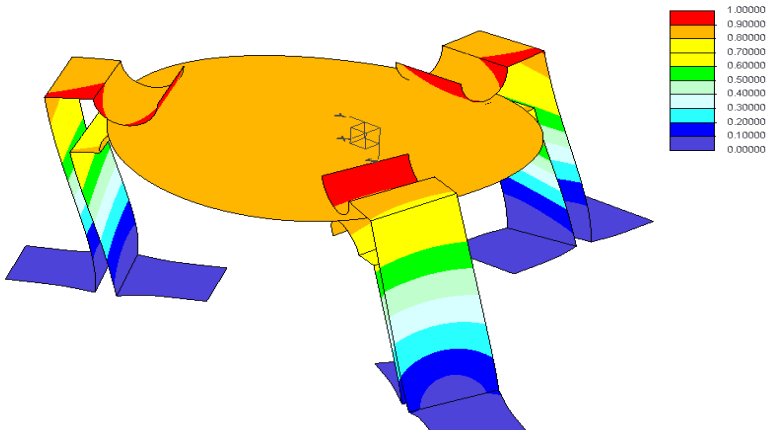

Figure 2-38 QCM 2nd vibration mode

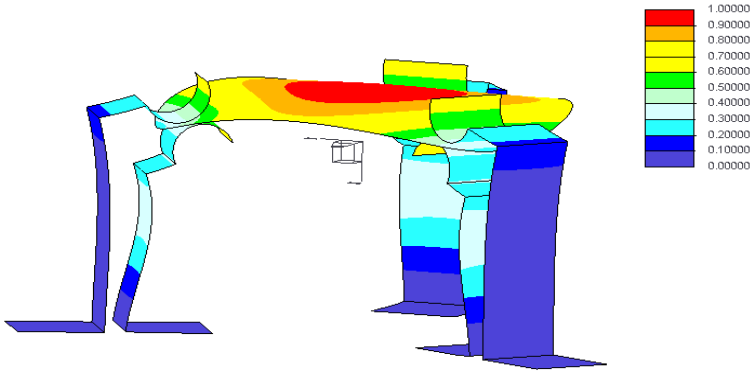

Figure 2-39 QCM 3rd vibration mode

Material	First mode [Hz]	Second mode [Hz]	Third mode [Hz]
Titanium alloy	1498.7	1499.3	1975.2
Aluminum Alloy	1361	1364	1817

Table 8 Computed Eigen frequencies, Modal analysis, circular area

2.6.5 Quasi-Static Analysis

In order to account for the sweep sine and random excitation, quasi-static loading of 500 m/s^2 has been applied to three different directions, X, Y and Z. The letter is the direction normal to the crystal plane. Analyses have been performed with both titanium and aluminum supports. The following figures show computed Von-Misses stresses along each direction and with both materials.

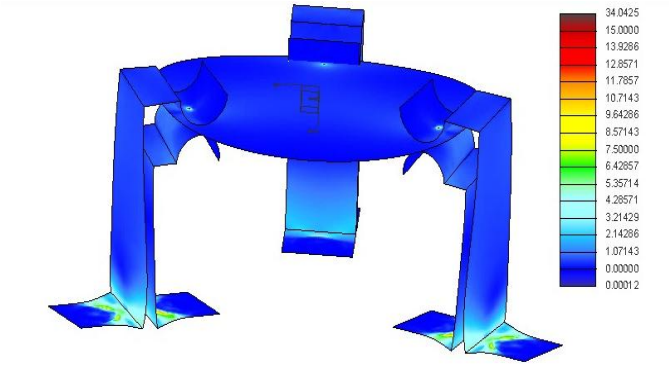

Figure 2-40 Von-Misses stress , Quasi-static loading on X direction

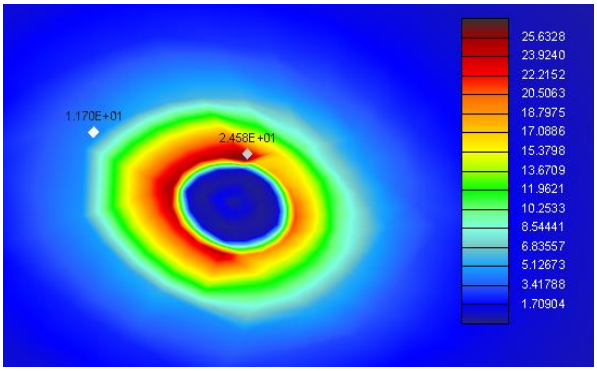

Figure 2-41 Zoom Near the link between the crystal and support

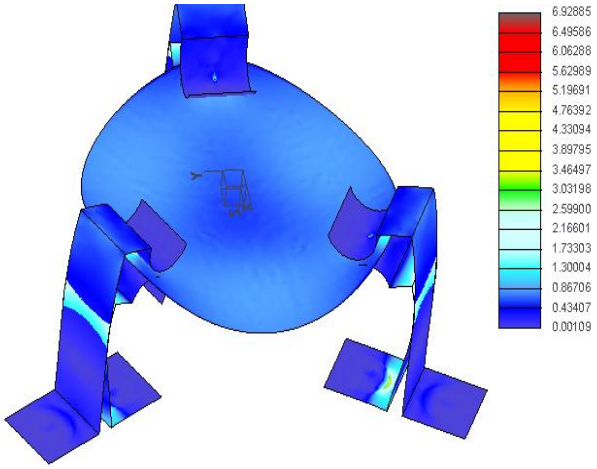

Figure 2-42 Von-Misses stress , Quasi-static loading along Y direction

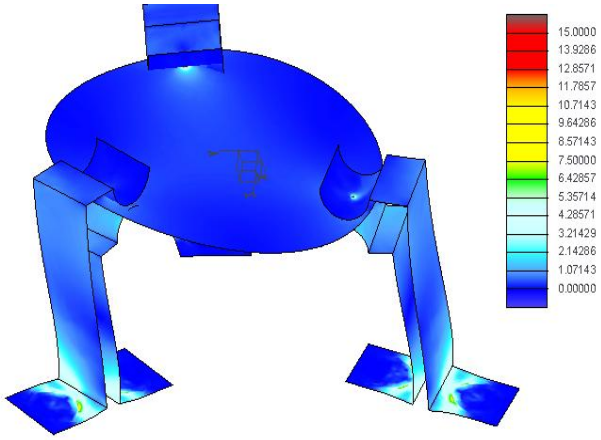

Figure 2-43 Von-Misses stress , Quasi-static loading along Z direction

Forcing direction	Material	Maximum Stress Quartz [MPa]	Maximum Stress Supports [MPa]	Modulus Quartz [MPa]	Modulus Supports [MPa]
X	Titanium	26.8	17.12	0.02	33
	Aluminum	23.5	13.5	0.14	24
Y	Titanium	25.3	15.6	0.07	36
	Aluminum	21.4	11.2	0.22	29
Z	Aluminum	4.2	3.4	0.85	169
	Titanium	4.4	3.6	0.84	92

Table 9 Summary of the Von-Misses stress in analyzed case

The analyses evidence that the worst case is the in plane loading (i.e. forcing along X and Y directions) and that the most critical component is the quartz crystal.The maximum stress is located at the connections between the crystal and the supports, as shown in figure (2-41).

The resulting stress derives from the distribution of the forcing at the connections and can be improved increasing the contact area and/or reducing the support stiffness. Both the approaches are suitable but the latter would lead to a reduction of the thermo-elastic stresses as well. Anyway, in all the cases acceptable modulus are derived.

2.6.6 Conclusions

The feasibility of the various configurations has been verified with thermo-elastic, modal and static analyses based on FE models.
The worst condition is generated by the thermo-elastic stresses due to the environment at -200°C and sensor regeneration. The analysis allow the solutions comparison of the mounting concepts but more accurate modeling of the contact regions between the supports and the crystal would be needed for the actual stress prediction in that area.The baseline for the contact geometry of the supports is the spherical one since it provides for lower stress around the contact areas and micro-sliding of contact surfaces is expect to be substantially smaller.
The dynamic behavior of the QCM is compliant with the usual stiffness requirements, providing first resonances well above 1000 Hz. This result allows reducing critical loading due not only to sine but also random excitations. Moreover, since there exist some margin w.r.t., the dangerous spectral region, Eigen-frequencies can be reduced in case more compliant supports would be needed. The stiffness can be easily tuned by changing the bending stiffness of the supports, for instance changing their thicknesses. This can allow reducing the thermo-elastic stresses within the quartz crystal in the expected thermal environment or conversely to increase the first natural frequency.
Finally, quasi-static analyses did not evidence criticalities for both the crystal and the supports. The most critical loading is the one acting in the crystal plane. Anyway, the stress can be tuned by acting on the supports' geometry, i.e. increasing the contact area with the crystal. This would lead to a stress reduction over the crystal. However, a trade-off with thermo-elastic stresses must be performed

3 Design and Manufacturing of Damping System

3.1 Need of Dampers

Dampers by design are adjustable and versatile elements since they include internal elements, which can be tightened by the help of the threaded damper cap. This specific characteristic allows for the modifications of damper properties such as stiffness and damping in a wide range.

This unique characteristic highlights the task of tuning the dampers in order to achieve an optimum dynamic behavior. In our study this objective mainly accomplished by determining the optimum preload.

The quartz crystal microbalance will be mounted on a damping system in order to reduce the amplitude of the mechanical vibrations, which are produced by the environmental and landing condition. They may suggest two types of vibrations acting on the microbalance, the *Sine* and the *Random* vibration.

In order to inhibit the probable distraction and failure of the microbalance by these two stimulus it is needed to design a damping system to dissipate the generated energy. This system must respect the characteristic of the microbalance in terms of mass of the supports and springs, stiffness of the elements and natural frequency of the microbalance.

Having thenatural frequency of the microbalance greater than 1kHz, Interval of the sweep sine excitation and random excitation and the practical working temperature interval of -150°C to 200°C are main factors in design of the vibration absorbing system.

Considering the interval of the random frequency applied on the microbalance starting from 20 [Hz] up to 2000 [Hz], simply it is possible to calculate the standard acceleration from the equation below which is called *MilesEquation*. As it is discussed in previous sections, it is needed to respect the magnitude of 50*g for the acceleration.

This equation is attributed to John. W. Miles

$$G_{RMS} = \sqrt{\frac{\pi}{2} . f_n . Q . [ASD_{input}]} \quad (3.1)$$

G_{RMS} = Root mean square acceleration in g's.
f_n = Natural frequency
Q=1/ζ Transmissibility (or amplification factor) at Natural Frequency
ζ = Critical damping Ratio
ASD_{input} = Input acceleration spectral density at f_n . [g^2/Hz]

Miles equation in general can be used for two main purposes.

1. During the design of a part, if enough analysis has been performed to determine the part has a predominant resonant frequency, then Miles' Equation can be used to estimate the loads due to random vibration. Just calculate the G_{RMS} value and multiply it by 3. That's the "three-sigma" load.
2. The accelerations due to random vibration at resonant frequencies in a multiple degree of freedom system can be approximated using Miles' Equation. This will indicate how much of the overall RMS acceleration is occurring at a resonant peak of interest compared to the complete frequency spectrum and this purpose is our case of interest in this chapter.

As it is discussed before since the peak response is not precisely known, the rule of thumb is to look at 3*standard deviation. By this way if the maximum response was predicted to be 10*g [m/s^2] then the 3*peak response is 30*g [m/s^2].

To figure out how does the system respond to the environmental condition during landing vibrations, it is considered a range of frequency by which is calculated the related input ASD in order to have the Miles acceleration.
Using the iteration method to calculate the Miles acceleration according to the desired natural frequency of 1kHz, the calculated ASD from the input frequency range of interest (20 [Hz] to 2000 [Hz]) and the arbitrary range for the damping ratio, helps us to understand how much will be the desired damping ratio by which the calculated mile acceleration is kept lower than 50*g.

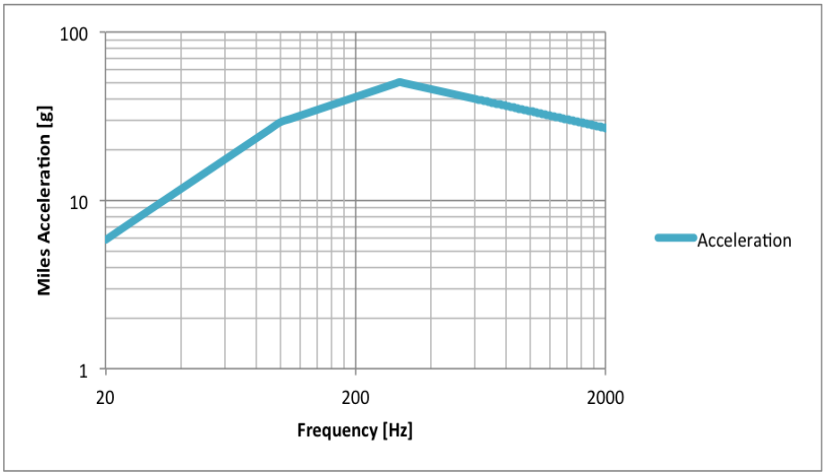

Figure 3-1 Mile Acceleration in Frequency range of interest

Looking at the calculated Miles acceleration through the frequency rate of interests and the related ASD_{input},verifies that in order to keep the acceleration below 50*g, it is needed to have an active damping system.

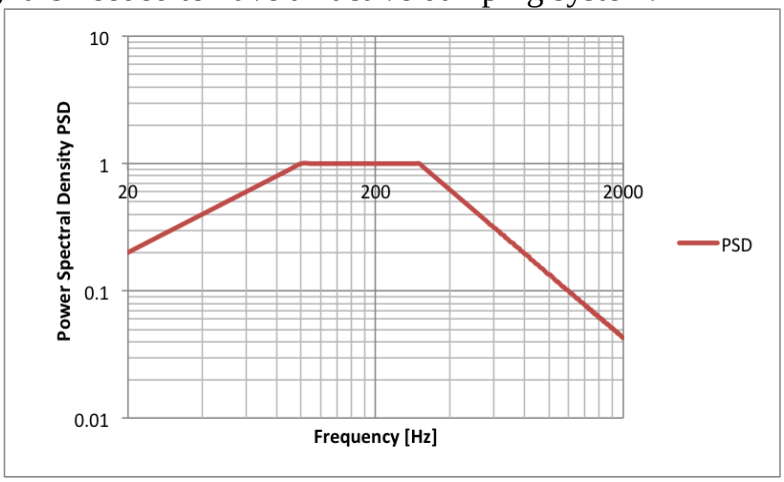

Figure 3-2Power Spectral Density in Frequency Range of interest

In order to design a damping system with high value of damping characteristics, there are several important factors, which needs to be considered in microbalance system. Among them the material used in damping system is so important, cause it is needed to apply the damping effect in a specific working temperature interval, which is a cryogenic temperature interval.

So finding such a material that can resist between -150°C up to 200°C and can apply the requested damping effect properly is the first objective of the design step.

Following on it is required to calculate precisely how much is the desired damping ratio of the damping system. So first it is needed to know what is the response of the microbalance to the applied stimulus during landing. The main idea of finding the response of every system to an arbitrary input is using the frequency response functions (FRF).

Frequency Response Functions are normally used to describe the input-output relationship of any system.

$$H\ (w) = \frac{Y\ (w)}{x\ (w)} \qquad (3.2)$$

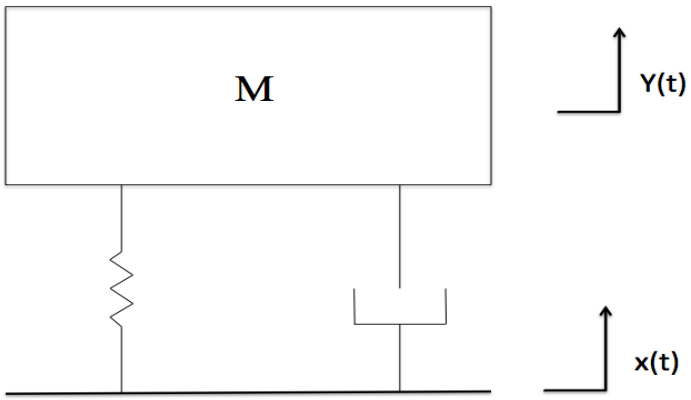

Figure 3-3The basic Frequency Response Function used throughout the study as a ratio of measured acceleration

3.1.1 FRF definition

Suppose a one-degree of freedom system with given mass *m*, stiffness coefficient *k and* damping coefficient *c*. The equivalent system with these properties representing the test setup is shown in figure (3-2).

x(t) denotes the known displacement of the support while Y(t) denotes the absolute displacement of the mass. The equation of motion governing such a system is then given by:

$$my + c\dot{y} + k\ddot{y} = c\dot{y} + kx \quad (3.3)$$

Then in order to describe a relation between the input and the output of the system, the frequency response must be defined:

$$H\ (jw) = \frac{Y}{X}$$

To express the frequency response, the time variables are transformed into frequency domain:

$$y(t) = Y\, e^{jwt}$$

$$\dot{y}(t) = jw.Y\, e^{jwt}$$

$$\ddot{y}(t) = -w^2.Y\, e^{jwt}$$

$$x(t) = X\, e^{jwt}$$

$$\dot{x}(t) = jw.X\, e^{jwt}$$

Replacing these into the equation of motion and simplifying

$$m(-w^2 Y e^{jwt}) + c(jwY e^{jwt}) + k(Y e^{jwt}) = c(jwX e^{jwt}) + k(X e^{jwt})$$

$$(-w^2 m + jwc + k)Y e^{jwt} = (jwc + k)X e^{jwt}$$

Finally, the frequency response describing the relationship between the input and the output of the system can be written as

$$H(jw) = \frac{Y}{X} = \frac{jwc + k}{-w^2 m + jwc + k} \quad (3.4)$$

The frequency response function is a complex function that can also be described in terms of its magnitude and phase:

$$G(w) = |H(jw)| = \frac{Y}{X} = \left|\frac{jwc + k}{-w^2 m + jwc + k}\right| \quad (3.5)$$

$$\varphi(w) = \arg\big(H(jw)\big) = \frac{Y}{X} = \arg\left(\frac{jwc + k}{-w^2 m + jwc + k}\right) \quad (3.6)$$

Here Y/X is calculated as the ratio of the absolute displacement of the mass to displacement of the base. However, multiplying the numerator and denominator of this ratio by w^2 shows that *H(jw)*also represents the ratio of the absolute acceleration of the mass to the acceleration of the base. This result is important since for all the tests regarding this study, the reference input and the measured output is in terms of acceleration.
The FRF can be rewritten in terms of the damping ratio:

$$\xi = \frac{C}{C_{cr}} = \frac{C}{2\sqrt{km}} \quad (3.7)$$

$$H\ (jw) = \frac{w_0^2 + 2jw\xi w_0}{(w_0^2 - w^2) + 2jw\xi w_0} \quad (3.8)$$

3.2 Design of Dampers

It is known that for a linear single degree of freedom system, the stiffness and the natural frequency are correlated with the expression:

$$w_0 = \sqrt{\frac{K}{m}} \quad (3.9)$$

Where w_0 is the natural frequency in [rad/s], k is the stiffness coefficient and m is the mass of the system connected to the spring.

The environmental and landing conditions suggest a sinusoidal excitation with amplitude of maximum 25 g. Therefore, the damper must be designed and its parameters characterized at this vibration level.

The sine environment is more significant at low frequencies (below 100 Hz) while the random one is more critical above 100 Hz.

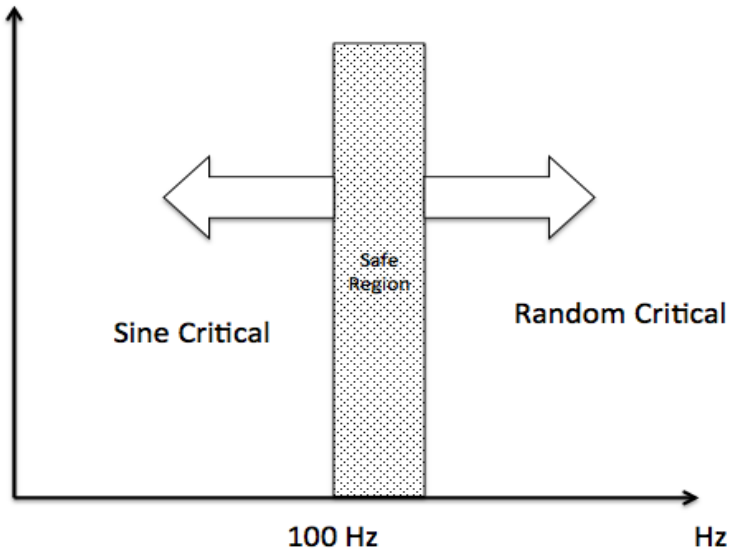

Figure 3-4The critical sine and the random vibration environment

The characterization of the damper requires a determined stimulus as the reference input. There exist two types of inputs. A signal driving by the shaker is generated and controlled in a closed loop feedback system by the control PC. Sweep signal is another test input, which is a sine signal with constant amplitude and increasing frequency at a constant logarithmic rate. (Usually defines as octaves/min). This provides a good method to excite a wide band of frequency in a small amount of time as our sinusoidal stimulus.

In order to start with the design calculation it is necessary to explain briefly the calculation path and algorithm.

Damping and stiffness are kept as free parameters to get the output response both with sweep sine and random excitation. The objective is to identify stiffness and damping regions where the maximum acceleration amplitude is lower than the 500 m/s^2 design value.

Thus, we are going to analyze the variation of Mile acceleration with respect to the inputs to find an interval of the resonant frequency in which the amount of the calculated acceleration is kept lower than 50g, as it is discussed before.

For the first step according to the design information and practical conditions it is calculated, the number of octaves /cycles for each input frequency in order to evaluate the related PSD. Meanwhile according to the following formula it is needed to calculate the transmissibility and the argument of it by using the iterative method for each input frequency.

$$G(w) = |H\ (jw)| = \frac{Y}{X} = \left|\frac{jwc + k}{-w^2m + jwc + k}\right| \qquad (3.10)$$

$$\varphi(w) = \arg\big(H\ (jw)\big) = \frac{Y}{X} = \arg\left(\frac{jwc + k}{-w^2m + jwc + k}\right) \qquad (3.11)$$

Regarding that it is prepared an script by Matlab which calculates the Magnitude of Frequency response function and its argument for the Input frequency range of interest, natural frequency range of interest which is identical to the input frequency range and the arbitrary range for the damping ratio.

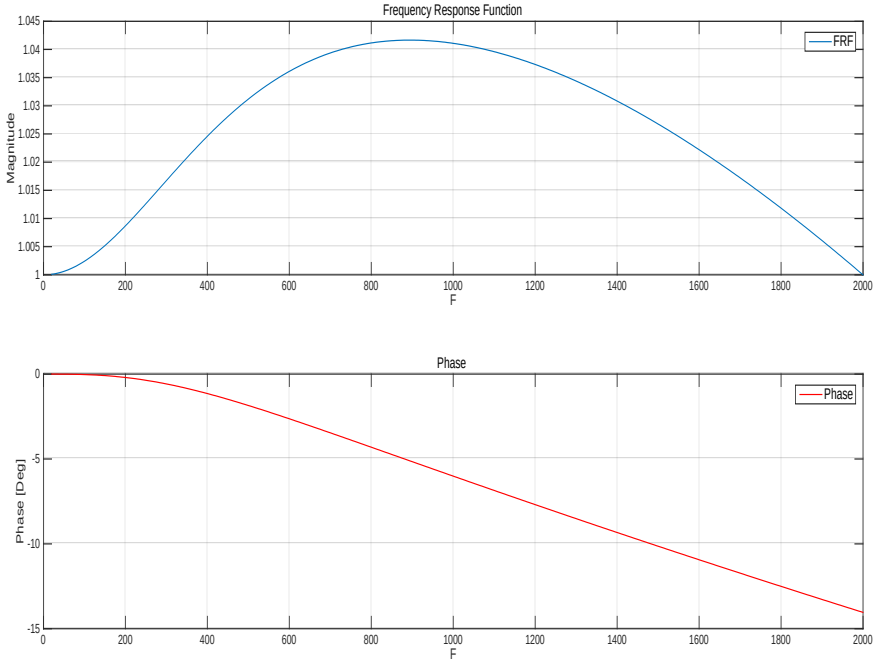

Figure 3-5 FRF and Phase Diagram

Having the FRF and its argument helps us to calculate the response of our system to each arbitrary excitation input. Thus multiplying the arrays of our PSD random excitation in to the squared of transmissibility function and the sweep sine input matrix into the transmissibility leads to have the weighted output PSD and the output swept sine, as it is shown in the following figures.

Sweep sine and Random excitation inputs and the expected response plot of the damped system is shown in following figures.

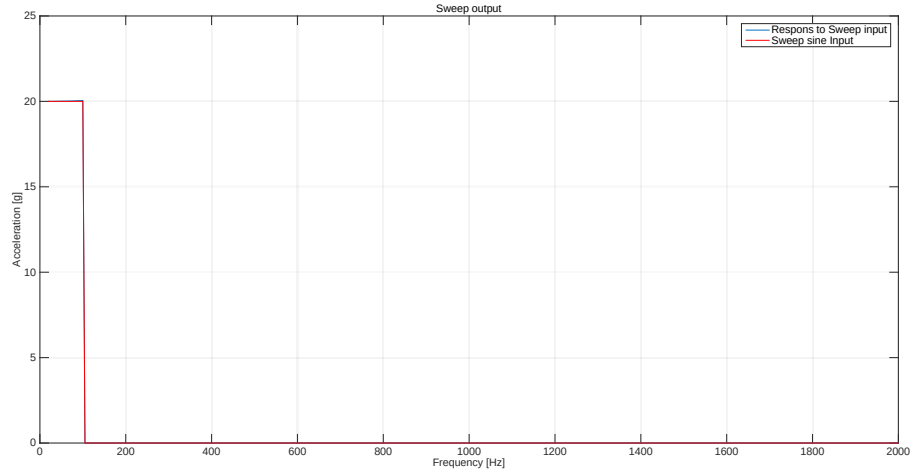

Figure 3-6 Sweep sine input stimulus and expected output respond

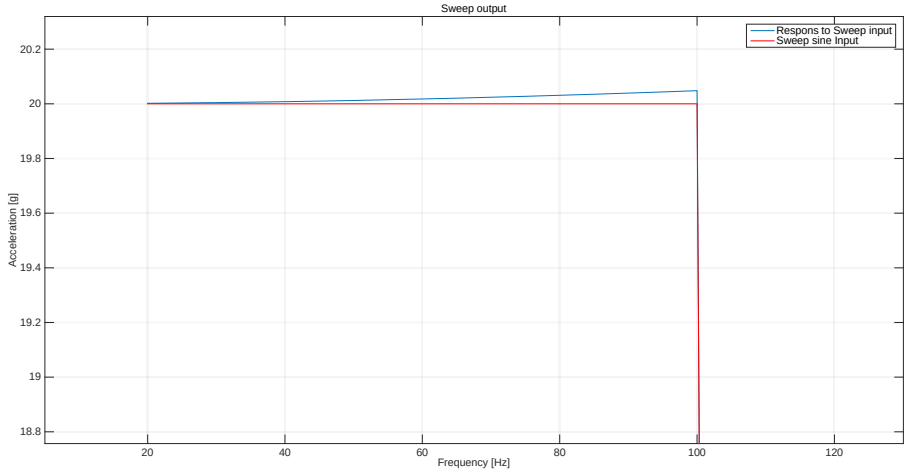

Figure 3-7 Sweep Sine input stimulus and expected output respond

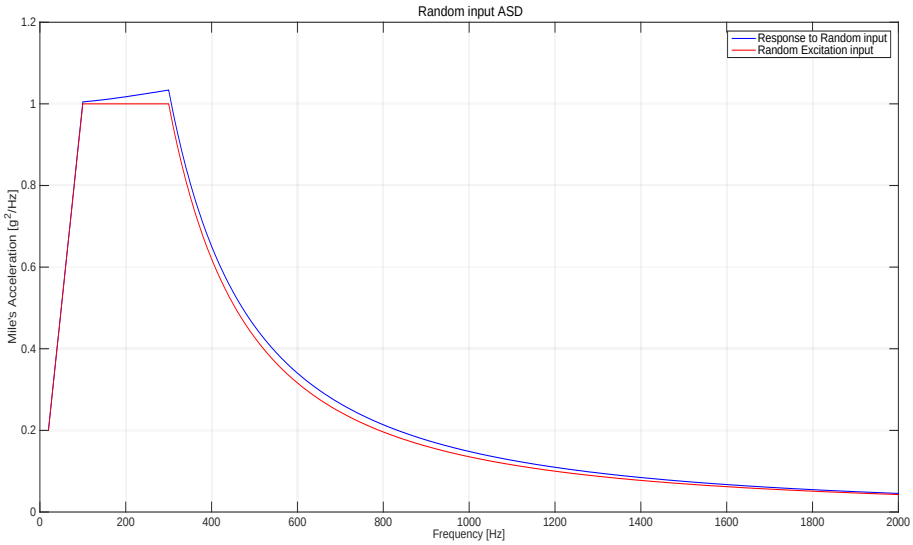

Figure 3-8 Random Excitation input and expected output diagram

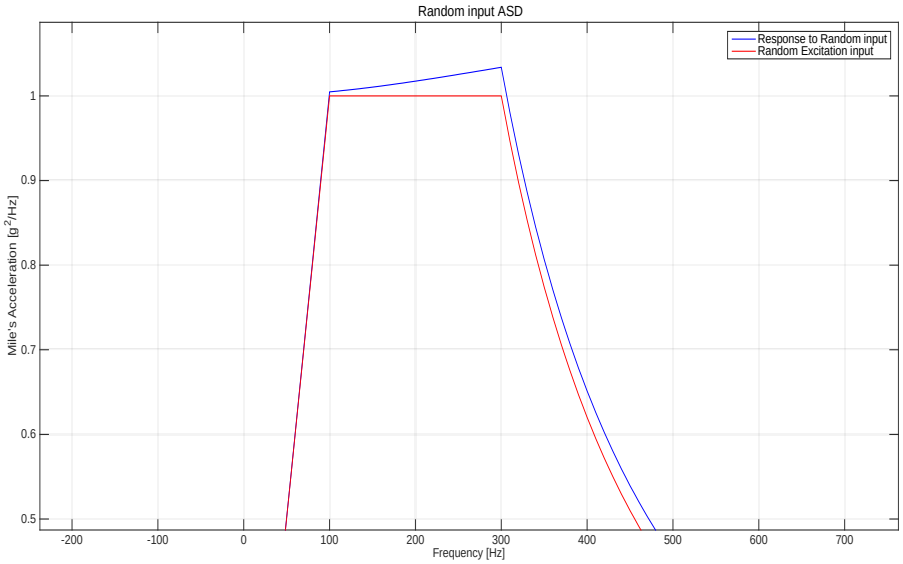

Figure 3-9 Random Excitation input and expected output diagram

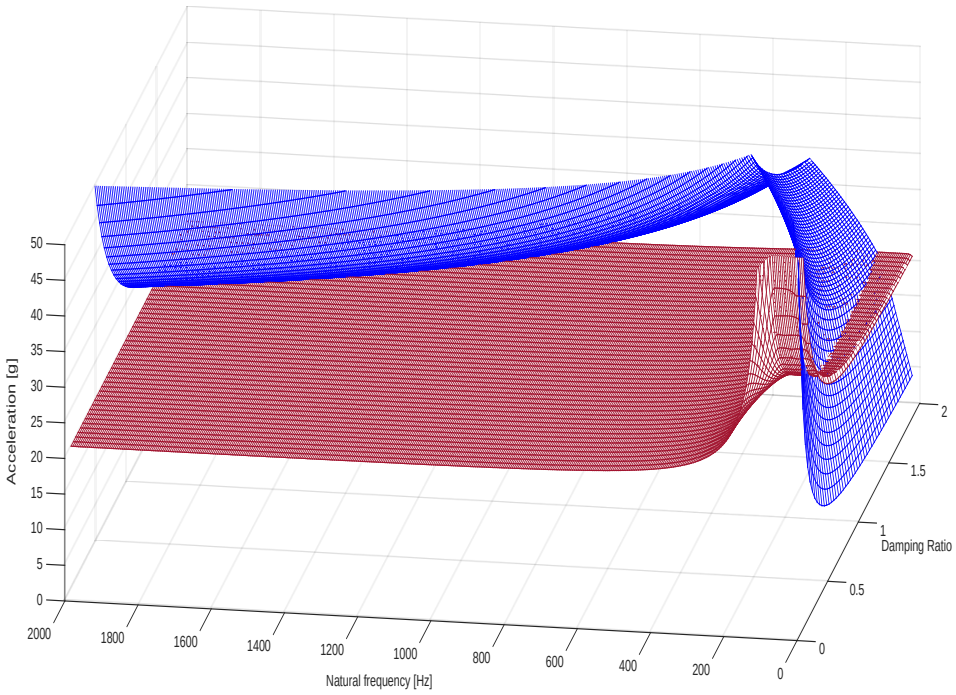

Figure 3-10 Three Dimensional graph of the expected output for the Random PSD input (Blue) and swept sine (red)

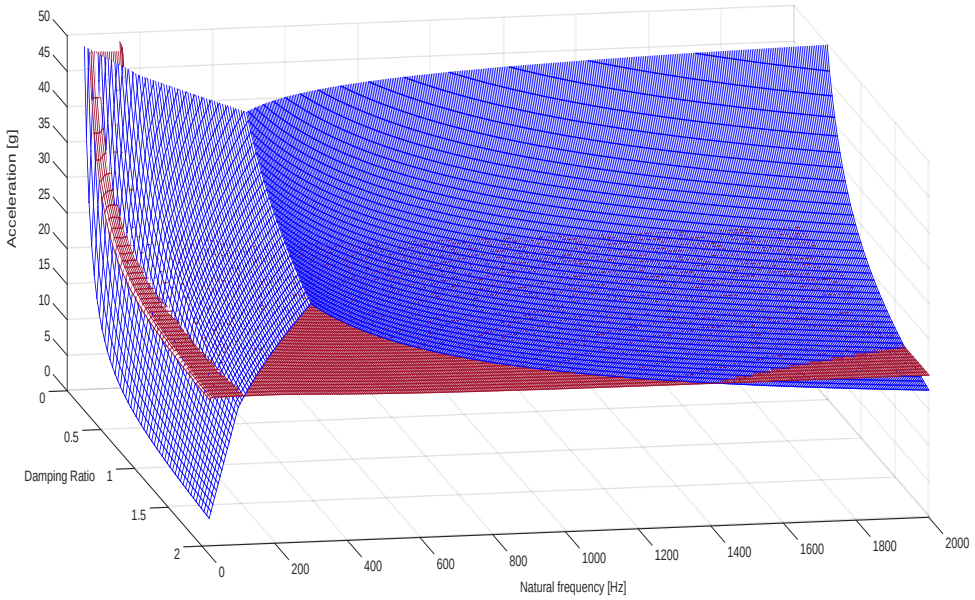

Figure 3-11 Three dimensional graph of the expected output for the random PSD (Blue) and Swept sine (red)

Several important results are achieved from the evaluated data and graphs.
First, from the evaluated three dimensional acceleration graph with respect to the Random excitation of input frequencies and damping ratios and comparing it with the output results from the sweep sine input, it is clearly obvious that having the damping ratio **less than 0.5** which is equal to the factor of quality of less than 1, leads to cross the border of acceleration equal to 50g [m/s^2] as a limit.

Another important issue related to the resulted three dimensional graph of the equivalent acceleration,with respect to the Random excitation of input frequencies and the damping ratio, is considering that the natural frequency of the total microbalance system is equal to 1.4 kHz, a precise look on the border that two output graphs crossing each other is a guide line to figure out the practical and functional range of the natural frequency, in which our damping system should be designed based on it.

Thus in order to keep the acceleration below 500 m/s^2 and regards to the natural frequency of the microbalance, which is equal to 1.4 kHz, the damping ratio is needed should be **at least $\zeta = 0.50$** and the natural frequency of the damper element has to respect the interval of **40Hz** up to **130 Hz**.

As it is discussed before the sweep sine excitation input is working on the interval of 20 Hz up to 100 Hz, thus it is needed to subtract this zone from the considered interval so by the end of the day the natural frequency of the damper element has to respect the interval from 100 Hz up to 130 Hz.

$$100\ [Hz] < f_n < 130\ [Hz]$$

3.3 Damping system solutions

According to the results and the evaluated data from the analytical and mathematical calculation it is needed to design a damperin order to prevent development of the vibrations. Two techniques are used to solve these vibration control problems, modifying stiffness or the natural frequency of the components, and their damping.

These solutions are often correlated to each other. An increase of stiffness results in reduction of deformations of the component or in reduction of relative motions between the components. These effects usually lead to damping reduction in the stiffened component, since energy dissipation constituting the damping effect results from deformations and relative displacements between the components of a damping system.

Thus, modifications aimed to enhance stiffness, may in the same time fail in controlling vibrations due to reduction of damping.

It is important to understand, how much stiffness can be enhanced without loosing too much damping capacity of the damping system. Increase of the fundamental natural frequency is usually achieved by increasing stiffness, although in some cases also by reducing the effective mass of the system.

As previously mentioned the dampers are highly non-linear elements. This means that their behavior is strongly depends on the magnitude of the incoming stimulus. The fact that the excitation amplitude affects the natural frequency is phenomenon that must be taking into consideration during design step.

In the following section two types of damping systems are proposed, which are analogous in some cases. Both of them are known as new categories of dampers. Definitive characteristics are compared in both cases and the consequence is prepared at the end of the section, grants the designer to make a decision.

3.4 Introduction to integrated support-damper of Metal Rubber[46]

Metal Rubber (MR) is a commercially available material used in a variety of applications, such as sealing, filtering and vibration absorbers. Metal rubber was first used as a rotor- dynamic damper in parallel with elastic bearing in cryogenic fuel turbopumps.

NitinolMetal Rubber (SMA-MR) displays a strong shape memory effect and temperature-dependent mechanical characteristics when subjected to specific heat treatment.

MR dampers have been evaluated to solve rotordynamic stability problems in the space shuttle main engine fuel turbo-pump. Other researchers have also attempted to identify the nonlinear quasi-static stiffness and damping coefficients in MR dampers, and to improve their mechanical characteristics.

Figure shows the prototype of the SMA- MR damper.The support damper is made from outer and inner steel rings and eight SMA-MR elements assembled at equal circumferential spacing of 2mm.

The SMA-MR elements work as elastic supports that also provide energy dissipation from the *material structural damping* and *dry friction* between the MR and the ring slots. The SMA-MR elements, a compressed weave of metal wires, are fabricated using the *Nitinol shape memory alloy coil wires* through the weaving and compression molding procedures.

Quasi-static tests of the SMART MR specimens show the linearity of the stiffness within a strain range up to 2%, which confirms the substantial validity of the use of the linear model as a first approximation to identify the dynamic properties of the SMA- MR devices with small vibration amplitudes.

The smart MR damper exhibits variable stiffness with softening response against the vibration amplitude, but with increasing stiffness coefficients at 90°C and significant values of loss factors at all temperatures. This is the first time that an integrated support damper made from SMA-MR is designed and evaluated in its static and dynamic characteristics, as well as against the variation of the environmental temperature.

3.5 Nonlinear Static and Dynamic Properties of Metal Rubber Dampers[47]

Metal Rubber (MR) is a form of a metallic mesh that is manufactured via a process of wire drawing, weaving and compression molding. The term Metal Rubber arises from the similarity between the properties of MR and those of rubber. MR can provide useful levels of damping at both low and high temperatures making it a strong candidate for applications in extreme environments.

The effective Poisson's ratio for MR is also obtained based on both compression and tensile tests. Dynamic properties of MR are characterized using the rigid body mode of a stiff tube supported by MR elements by applying different levels of dynamic strain amplitude and frequency. Dynamic hysteresis loops are also examined from blocked-force measurements on MR specimens. A comparison is made between the properties of MR and a silicone elastomer.

3.5.1 Dry Friction Properties of MR Dampers

The structure of a MR damper is formed from tight coils of metal wire that are pressed and firmly entangled together. The stiffness is defined by the characteristics and the arrangement of the metal coils. Dry friction damping arises from movement between the metal wires and in the overall level is assumed to be controlled by the number of contact points, the pressure and friction at each point.

3.5.2 Overview

The stiffness and damping are affected by the structural parameters including its relative density, wire diameter and typical coil size.
MR displays strain dependent damping behavior. The dynamic stiffness of MR presents a strong nonlinear softening characteristic. Properties are also affected by the pre-compression and excitation frequency.
Compared to an elastomeric material, MR can provide improved damping at higher excitation levels. Some similarity exists between the hysteresis loops and as a first approximation, a complex modulus type model commonly used with viscoelastic materials may be adequate.

4 Conclusions

In this study, preliminary sketch, characterization and optimization process of a holding system designed for a quartz crystal microbalance devoted to a Mars explorer was realized by the computational methods. In order to reach the proposed goal several integrated objectives were pursued instantaneously.

In the optimum configuration, the microbalance is designed by three supports plus three springs which are positioned symmetrically by 120° with respect to each other. The support material is of titanium alloy (Ti-6Al-4V) but usage of aluminumalloy has been investigated as well. A lightweight durable structure has been designed.
Finite element analyses have been performed to validate the preliminary mechanical design. Results ensure the integrity of quartz when the microbalance is exposed to the acceleration of 500 m/s^2, proper mechanical behavior and resistance against thermo-elastic stresses induced during regeneration phases, i.e between -200 and 200 °C. Three significant modes of vibration were observed at frequencies above 100 Hz, so a positive result regarding the environmental condition. These analyses showed that the first natural frequency of the holding system is around 1490 Hz.

The high excitation levels due to random forcing at the rocket landing required the design of a damping system.
As evaluated by numerical calculation there exists an interval for the natural frequency of the damping system, which is needed to be far away from the Eigenfrequency of the microbalance. This interval starts from 40 Hz and ends up with 130 Hz beside to a damping ratio of at least 0.5. Under this prospective, the significant variability of the stiffness and damping properties at low and high temperatures of SMA-MR dampers is very promising for the active vibration control of the CAM project.
Future development of this work will be the design of the damping system for the CAM instrument and testing of the developed solution in representative mechanical and thermal environment.

5 Annex A

5.1 DAMPING Script

```
clc
clear all
close all
%% parameters definition
fn   =  20:5:2000;                  % Natural Frequency [Hz]
wn   =  2*pi*fn;
ksiv =  linspace(0.1,2,50);         % Damping Ratio
f    =  20:5:2000;                  % Random  input frequency
w    =  2*pi*f;
%% Input PSD
PSDm=xlsread('datathesis');
PSDint=interp1(PSDm(:,1),PSDm(:,2),f);
%% Input Sweep
for ii=1:length(f)
if(f(ii)<=100)
sweep(ii)=20;
else
sweep(ii)=0;
end
end
%% index of 1k
for ii=1:length(f)
if(f(ii)<1000)
else
ind1k=ii;
break
end
end
fn1k=1000; % resonance
% plot(f,sweep);
% grid on
%% Solutions
for bb=1:length(w)
forjj=1:length(ksiv)
wn=w(bb);
fn=w(bb)/(2*pi);
ksi=ksiv(jj);
      Q=1/(2*ksiv(jj));
      H =(wn^2+1i.*2.*w.*ksi.*wn)./((wn^2-w.^2)+1i.*2.*w.*ksi*wn);
      %H = 1./(sqrt(((1-w/wn.^2).^2)+(2*ksi.*w/wn).^2));
      G=abs(H);
phi=angle(H)*(180/pi);

      % Random
PSDo=PSDint.*H.^2;
PSDm=abs(PSDo(bb));
Mileacc(bb,jj)=3*sqrt(pi/2.*fn.*PSDm.*Q);
      % Sweep
PSDso= sweep.*H;
PSDms(bb,jj)=max(abs(PSDso));
```

```
% Random 1k
      PSDm1k=PSDo(ind1k);
      Q1k=1/(2*0.05);
Mileacc1k(bb,jj)=3*sqrt(pi/2.*fn1k.*PSDm1k.*Q1k);

end

end


%% display solutions

figure(1)

plot(f,abs(PSDo),f,abs(PSDint))
title(' Random output');
xlabel('Frequency [Hz]');
ylabel('g^2/Hz');
grid on
legend({'Response to Random input','Random Excitation input'},'FontSize',14)

figure(2)
plot(f,abs(PSDso),f,abs(sweep))
title('Sweep output');
xlabel('Frequency [Hz]');
ylabel('g');
grid on
legend({'Respons to Sweep input','Sweep sine Input'},'FontSize',14)


figure(3)
subplot(2,1,1)
plot(f,H)
title('Frequency Response Function');
xlabel('F');
ylabel('Magnitude');
grid on
legend({'FRF'},'FontSize',14)
subplot(2,1,2)
plot(f,phi)
title('Phase Lag')
xlabel('F')
ylabel('Phase [Deg]')
hold on
grid on
legend({'Phase'},'FontSize',14)

figure(4)
mesh(ksiv,w/(2*pi),Mileacc)
xlabel('Damping coefficient');
ylabel('Natural frequency [Hz]');
zlabel('Miles acceleration [g]');
zlim([0 50]);
hold on
mesh(ksiv,w/(2*pi),PSDms)
```

6 References

[1] Cady, W.(1947). Piezoelectricity. 1946

[2]Curie, J. ,& Curie, P. (1880). An oscillating quartz crystal mass detector.Rendu, 91, 294-297.

[3]Lippman,G. (1881). Sur le principe de la conservation de l'electricite,ou second principe de la theorie des phenomeneselectriques. Comptrendus, 92, 1049-1051.

[4] Sullivan, D. (2001). Time and Frequency measurement at NIST: The first 100 years. *Frequency Control Symposium and PDA exhibition*, 2001.*Proceeding of the 2001 IEEE International*, pp. 4-17.

[5]Bottom,V . E. (1981). A history of the quartz crystal industry in the USA.*Thirty Fifth Annual Frequency Control Symposium. 1981*, pp. 3-12.

[6] Sauerbrey, G. (1959). Use of quartz vibration for weighing thin films on a microbalance.J.Physik, 155, 206-212.

[7] Bottom, V.E. (1982). Introduction to quartz crystal unit design Van Nostrand Reinhold.

[8]Lu, C., &Czanderna, A. W. (1984). Applications of piezoelectric quartz crystal microbalances. Elsevier Science Publishers, 1984, , 393.

[9] Bottom, V.E. (1982). Introduction to quartz crystal unit design Van Nostrand Reinhold.

[10] Bottom, V.E. (1982). Introduction to quartz crystal unit design Van Nostrand Reinhold.

[11] Heising, R.A. (1946). *Quartz crystals for electrical circuits, their design and manufacture*D.VanNostrandcompany, inc.

[12]Noel, M.A.M.,&Topart, P .A. (1994). High-frequency impedance analysis of quartz crystal microbalances. 1. General considerations. *Analytical Chemistry*, 66(4), 484-491.

[13] Stockbridge ,C. (1966). Vacuum microbalance techniques. Vol.5 Plenum, New York, , 193.

[14] Benes,E. (1984). Improved quartz crystal microbalance technique. *Journal of applied physics*, 56(3), 608-626.

[15] Hlavay,J., &Guilbault, G. G. (1977). Applications of the piezoelectric crystal detector in analytical chemistry. Analytical Chemistry,49(13), 1890-1898.

[16] Sauerbrey, G. (1959). Use of quartz vibration for weighing thin films on a microbalance.J.Physik, 155, 206-212.

[17] Wimmer,K.,Hertl, S.,Hemetsberger,J.,&Benes,E.(1984). New method of measuring vibration amplitudes of crystals. Review of scientific instruments, 55(4),605-609.

[18] Benes,E. (1984). Improved quartz crystal microbalance technique. *Journal of applied physics*, 56(3), 608-626.

[19]Lu, C. (1975). Mass demonstration with piezoelectric quartz crystal resonators. Journal of vacuum science and technology,12(1), 578-583.

[20] Reed, C., Kanazawa, K. K., & Kaufman, J. (1990). Physical description of a viscoelastically loaded AT-cut quartz resonator. Journal of applied physics, 68(5).

[21] Benes,E. (1984). Improved quartz crystal microbalance technique. *Journal of applied physics*, 56(3), 608-626.

[22] Josse,F.,Lee,Y.,Martin,S.J.,&Cernosek, R.W.(1998). Analysis of the radial dependence of mass sensitivity for modified-electrode quartz crystal resonators.*Analytical Chemistry*, 70(2),237-247

[23]Buttry,D.A.,&Ward,M.D.(1992). Measurement of interfacial processes at electrode surfaces with the electrochemical quartz crystal microbalance. Chemical Reviews, 92(6)

[24] O'sullivan.C.,&Guilbault, G. (1999). Commercial quartz crystal microbalances-theory and applications.*Biosensors and Bioelectronics*, 14(8), 663-670.

[25] Bottom, V.E. (1982). Introduction to quartz crystal unit design Van Nostrand Reinhold.

[26] Kanazawa, K.K.,& Gordon, J. G. (1985). Frequency of a quartz microbalance in contact with liquid.*Analytical Chemistry*,57(8),1770-1771.

[27] Reed, C., Kanazawa, K. K., & Kaufman, J. (1990). Physical description of a viscoelastically loaded AT-cut quartz resonator. Journal of applied physics, 68(5).

[28]Lin,Z., Yip,C.M.,Joseph, I. S.,& Ward, M. D. (1993). Operation of an ultrasensitive 30-Mhz quartz crystal microbalance in liquids.*Analytical Chemistry*, 65(11),1546-1551.

[29]Martin,B.A., & Hager, H.E. (1989). Velocity profile on quartz crystals ascillating in liquids.*Journal of applied physics*, 65(7),2630-2635

[30]Klavetter,E.,Martin, S.,&Wessendorf,K.(1993). Monitoring jet fuel thermal stability using a quartz crystal microbalance. Energy & Fuels,7(5),582-588.

[31] Yao,S.Z.,& Zhou, T.A. (1988). Dependence of the ascillation frequency of a piezoelectric crystal on the physical parameters of liquids.*AnalyticaChimicaActa*, 212, 61-72.

[32]Nomura, T., &Okuhara,. (1982). Frequency shifts of piezoelectric quartz crystals immersed in organic liquids.*AnalyticaChimicaActa*, 142, 281-284.

[33]EerNisse, E. (1972).Simultaneous Thin-Film stress and Mass-Change measurements using quartz resonators.*Journal of applied physics*, 43(4),1330-1337

[34] Elam,J.,&Pellin, M.(2005). GaPO4 sensors for gravimetric monitoring during atomic layer deposition at high temperatures.*Analytical chemistry*, 77(11), 3531-3535.
[35] Girard, S., Gale, J . D., Mellot-Drazieks,C.,&Ferey , G. (2001). Derivation of interatomic potentials for gallophosphates from the GaPO4-quartz structure: Transferability study to gallophosphates and zeotypegallophosphates. *Chemistry of Materials, 13(5)*,1732-1738.

[36]Aziawa, H.,Inoue, Y., Yamanda, K., Hirata, M.,Koyama,M.,&Kurosawa,S.(2006). Resonant properties of GaPO4 resonator device coated with plasma polymerized stryne film. *International Frequency Control Symposium and Exposition, 2006 IEEE*, pp.318-321

[37]Engel,G., Krempl, P.,&Stadler, J.(1989). Technical aspects of GaPO4.*Proc. Of the 3rd European Frequency and Time Foroum (EFTF) , Besancon*, pp. 50-55.

[38]Krispel, F., Reiter, C., Neubig,J., Lenzenhuber,F.,Krempl , P., Wallnofer, W., et al. (2003). Properties and applications of singly rotated GaPO4 resonators.*Frequency Control Symposium and PDA exhibition jointly with the 17th European Frequency and Time Forum,2003 . Proceeding of the 2003 IEEE International*, pp.668-673.

[39] Thanner,H.,Krempl, P.W., Wallnofer, W.,&Worsch, P.M. (2002). GaPO4 high temperature crystal microbalance with zero temperature coefficient. Vacuum,67(3-4), 687-691

[40] Krispel,F., Reiter,C.,Schauperi, R., Mannelli, I., &Wallnofer, W. (2004) Microbalance sensor applications using the piezoelectric crystal material GaPO4. *Frequency and Time Forum, 2004. EFTF2004*. 18th European, pp. 565-568.

[41] Krempl,P., Krispel, F., &Wallnofer, W.(1997). Industrial development and prospects of GaPO4.*Annales De Chimie, ,* 22. (8) pp. 623-626

[42]Worsch, P. M., Krempl, P.W., &Wallnofer, W. (2002). GaPO4 crystals for sensor applications.*Sensors, 2002. Proceeding of IEEE, , 1* . pp. 589-593 Vol. 1.

[43] Palomba, E., Marra, C., Longobardo, A., Zinzi, A., Berazotti, A., Macagnano, A., et al. (2008). Volatile and organic content in regoliths: A device for in situ analysis. *37th COSPAR Scientific Assembley, ,* 37. pp.2334.

[44]Hibbeler, R. (1997). Mechanics of materials prentice hall international.

[45]http://www.crystran.co.uk/optical-materials/quartz-crystal-sio2

[46]Yanhong Ma1.,Qicheng Zhang., Dayi Zhang., FabrizioScarpa.,Baolong Liu.,Jie Hong. (2014). A novel smart rotor support with shape memory alloy metal rubber for high temperatures and variable amplitude vibrations.1 (2), 2-23.

[47]Hong Wang., J. A. Rongong., G. R. Tomlinson., Jie Hong. (2010) .Nonlinear static and dynamic properties of metal rubber dampers.1 (1) , 1302-1314 .